*Physics – Uspekhi* **48** (5) 469 – 486 (2005) 

*REVIEWS OF TOPICAL PROBLEMS* PACS numbers: **42.50. – p**, **84.47. + w**, 85.60.Gz

# Photocounts and laser detection of weak optical signals

V P Bykov

DOI: 10.1070/PU2005v048n05ABEH002103

## Contents



**Abstract. The nature of photocounts arising in detectors exposed to highly coherent laser radiation is discussed. It is shown that the spatial localization of a photon allowed in quantum electrodynamics fails to account for the effect observed and that the Coulomb instability of a low electron flux in a photodetector can be the explanation. With detectors utilizing nonfree electrons, namely, electrons bound in atoms, ions, molecules, etc., weak optical signals can be detected with laser radiation without photocounts, in other words, at a suppressed shot noise. A basic scheme for a laser detector using bound electrons is suggested.**

## 1. Introduction

Detection of light is one of the most fundamental physical processes playing an important role both in nature and technology. In nature, this process underlies vision, hence the ability to perceive the surrounding world. In technology, a variety of photodetectors is used to quantitatively describe the process of detection of optical signals and to extend the spectrum of the received radiation.

Despite considerable progress in the development of photodetectors, the understanding of fundamental processes underlying photodetection continues to be based on concepts dating back more than fifty years ago. This area of research turned out to be overshadowed by the impressive achievements of laser physics and has attracted little attention. At the same time, the creation of highly coherent laser sources resulted in a certain discordance between the former approaches to light detection and even turned it into somewhat of a mystery.

The concepts of photocounts and photons as spatially localized particles are closely interrelated. It is believed that a photon, a spatially localized particle (corpuscle), is absorbed when it enters a photodetector and produces a released electron; the electron spreads in the detector circuit giving rise to a splash in the electric current, termed the photocount.

These concepts remained practically unaltered for a very long time despite considerable changes in experimental physics and electromagnetic field theory. Suffice it to mention the enormous possibilities offered by the invention of lasers and the development of such theories as quantum mechanics and quantum electrodynamics (QED). Today, it is a well-established fact that quantum laws do operate in nature. Indeed, quantum electrodynamics is considered the most accurate physical theory, its corollaries having been verified to within a large number of significant figures following the decimal point. However, the concept of photons in the framework of QED and the concept of photons as a cause of photocounts are essentially different. This difference is thoroughly discussed in the present review.

**V P Bykov** A M Prokhorov General Physics Institute,
Russian Academy of Sciences,
ul. Vavilova 38, 119991 Moscow, Russian Federation
Tel. (7-095) 135 02 70
E-mail: v.p.bykov@mtu-net.ru

Received 3 November 2004
*Uspekhi Fizicheskikh Nauk* **175** (5) 495 – 513 (2005)
Translated by Yu V Morozov; edited by A Radzig

## 2. Physical nature of photocounts

### 2.1 The photocount as a physical phenomenon. The problem of photocounts updated

The physical nature of photocounts (pulses in the external circuit of a photodetector, with a characteristic length of

$\approx 10^{-8}$ s) had been a subject of research long before laser sources of radiation appeared [1]. As mentioned in the Introduction, they were primarily explained as a consequence of the release of an electron (particle) knocked out by a photon (particle) from the photocathode. The situation changed with the advent of lasers. Before that, the spectrum width of optical signals arrived at the cathode of a photodetector from thermal and luminescent sources was $\approx 10^{12}-10^{15}$ Hz. In other words, it was much greater than the characteristic spectral width $\approx 10^{8}$ Hz of the output signal from the detector, which is determined by the duration of current pulses in this signal, i.e., by the photocount length. The spectra of laser sources are far narrower than $10^{8}$ Hz; the record-breaking devices have a spectral width of only 1 Hz. Switching over to the detection of coherent laser signals has had practically no effect on the characteristics of the output signal which still remains a sequence of random pulses or photocounts of length $\approx 10^{-8}$ s. This means that the detection of a highly coherent signal reveals new frequencies in the spectrum of the photodetector output signal that could not be detected in optical signals in the days before the advent of lasers. The spectrum of a laser signal cannot change as it propagates through a vacuum which is an essentially linear medium. The photodetector being the sole source of nonlinearity, the broadening of the signal spectrum during the detection is unambiguous evidence that the cause of photocount occurrence is the detector itself rather than the received radiation.

The same problem can be formulated in a different way. The mysterious nature of photocounts mentioned in the Introduction may be illustrated by the diagram presented in Fig. 1. The highly coherent radiation fed to the detector input has a smoothly time-dependent amplitude whose typical variation time in good lasers measures a few seconds.

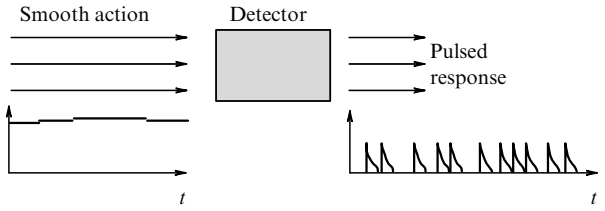


**Figure 1.** What is the cause of photocounts when a highly coherent signal enters the detector?

There is a sequence of pulses (photocounts) with a characteristic time on the order of $10^{-8}$ s at the detector output. It is natural to ask what the cause of these photocounts is? Such a question could not arise in the prelaser era because the light emitted from thermal and luminescent sources was chaotic and provided many causes for the appearance of photocounts.

There is voluminous literature on photocounts and their statistics (see, for instance, Refs [2–4]). However, the origin of photocounts and their nature is mentioned only incidentally [5] or not at all. As a rule, calculations using particular smoothly time-dependent characteristics of the field are performed and the result *is claimed* to refer to a flux of pulses, i.e., photocounts. But the nature of photocounts and their causative factors are virtually ignored.

The question posed earlier is understood to have three possible answers. The majority of researchers believe that radiation (coherent radiation in particular) contains spatially localized entities called photons that interact with the cathode of a photodetector and give rise to photocounts. Indeed, by *photocount statistics* is frequently meant *photon statistics*, having in mind spatially localized formations mentioned above. The scientific literature contains discussions of whether a photon flies after the interaction with a beam-splitting mirror, and so on.

Other researchers argue that the cause of photocount occurrence lies in the discrete nature of electrons. It is supposed that discrete electrons interact with a wave, the amplitude of which is smoothly time-dependent, and thus impart their discreteness to the response of the detector to radiation.

Finally, certain authors relate the appearance of photocounts to the so-called 'wave packet reduction' characteristic of quantum-mechanical measurements.

It will be shown in Sections 2.2–2.5 that none of these hypotheses can be regarded as valid in light of modern theories. This situation has been analyzed at length in a series of papers [6] where it is shown that the source of photocounts is the Coulomb instability of a low electron flux in the photodetector, induced by the received radiation. This instability is close to the Wigner instability [7]. Thus, photocount statistics is not photon statistics; rather, it largely reflects statistical properties of the breakdown of a low electron flux into separate bunches. This process is a manifestation of the instability said. Thus far, this is the sole approach free from controversy and explaining a wide circle of phenomena associated with photocounts.

Also, it will be demonstrated that the Coulomb instability can be avoided by using in photodetectors electrons bound in atoms, ions, and molecules, instead of free electrons. Light radiation laser detectors based on this principle have been proposed (see Section 3).

### 2.2 Photons from the standpoint of quantum electrodynamics

**2.2.1 What is a photon?** We shall address this question in the framework of modern QED or, to be more precise, based on the corollaries from the mathematical apparatus of QED.

Theoretical and experimental data are usually interpreted with reference to other notions, such, for example, as 'wave packet reduction', that supplement the QED mathematical apparatus. For the time being, we put these additional notions aside.

It follows from QED that an important feature of photons is their multifaceted character or the ability to appear in different representations. In what follows, two photon representations are considered: distributed and packet. The purpose is to clarify to what extent a photon can be regarded as a spatially localized entity.

**2.2.2 Distributed photon representation.** For photon description in QED, a large cubic resonator is normally introduced, in which the modes are plane waves with a discrete set of eigenfrequencies and wave vectors. From the quantum standpoint, such a mode is an oscillator and can be in states with different numbers of photons, as well as in other possible oscillator states (coherent, squeezed, etc.). When the oscillator is in a one-photon state, the photon field is uniformly distributed over the entire cavity volume. Because in field quantization the volume of a large cubic resonator finally tends to infinity, the photon field turns out to be uniformly

distributed over the entire infinite space. It is quite clear that such a photon cannot be the cause of a photocount since it lacks spatial localization. In a multiphoton state, there is no photon localization either because the total field of photons is uniformly distributed over the entire volume of the cavity, hence over the entire space, following the aforementioned passage to the limit. It can be concluded that photons introduced in this way are not localized and cannot account for photocounts.

Such a procedure of quantization of electromagnetic fields can be found in any QED textbook and is not described here. We shall borrow from it only the electric field operator having the form [8]

$$\mathbf{E}(\mathbf{r},t)=\frac{\mathrm{i}\sqrt{\hbar}}{2\pi}\sum_{\lambda}\int \mathrm{d}\mathbf{k}\ \sqrt{\omega}\,\mathbf{e}_{\lambda}(\mathbf{k})\,a_{\lambda}(\mathbf{k})\exp\left[\mathrm{i}(\mathbf{kr}-ckt)\right]+\text{H.c.}, \tag{2.1}$$

in which the summation is over two polarizations $\mathbf{e}_{\lambda}$; $a_{\lambda}^{+}(\mathbf{k})$ and $a_{\lambda}(\mathbf{k})$ are the densities of the creation and annihilation operators that obey commutation relation

$$a_i(\mathbf{k})\,a_j^{+}(\mathbf{k}')-a_j^{+}(\mathbf{k}')\,a_i(\mathbf{k})=\delta_{ij}\delta(\mathbf{k}-\mathbf{k}')\,, \tag{2.2}$$

and H.c. stands for a Hermitian conjugate expression of the preceding term.

**2.2.3 The photon as a wave packet.** For the packet representation [9], the creation and annihilation operators are introduced as follows

$$A=\sum_{\lambda=1,2}\int \mathrm{d}\mathbf{k}\ W_{\lambda}(\mathbf{k})\,\alpha_{\lambda}(\mathbf{k})\,,$$

$$A^{+}=\sum_{\lambda=1,2}\int \mathrm{d}\mathbf{k}\ W_{\lambda}^{*}(\mathbf{k})\,\alpha_{\lambda}^{*}(\mathbf{k})\,, \tag{2.3}$$

where $W_{\lambda}(\mathbf{k})$ is a certain normalized spectral function:

$$\sum_{\lambda=1,2}\int \mathrm{d}\mathbf{k}\ \left|W_{\lambda}(\mathbf{k})\right|^2=1\,, \tag{2.4}$$

which defines the packet spectrum (as shown below); $a_{\lambda}^{+}(\mathbf{k})$ and $a_{\lambda}(\mathbf{k})$ are the densities of the creation and annihilation operators entering expression (2.1) for the operators of the free-space electric field. It is easy to see that operators $A$ and $A^{+}$ obey the commutation relation

$$[A,A^{+}]=1\,. \tag{2.5}$$

Accordingly, operators $A$ and $A^{+}$ give rise to a system of steady states $|n\rangle$, such that

$$|n\rangle=\frac{(A^{+})^{n}}{\sqrt{n!}}|0\rangle\,,\qquad A|0\rangle=0\,. \tag{2.6}$$

An arbitrary state of such a packet can be represented in the form

$$|\Psi\rangle=\sum_{n=0}^{\infty}\Psi_n|n\rangle\,. \tag{2.7}$$

It can be shown that all averages are expressed through a single function that can be called the shape of the quantum wave packet. The average value of the electric field in state (2.7) is given by

$$\left\langle\mathbf{E}(\mathbf{r},t)\right\rangle=\mathbf{\Phi}(\mathbf{r},t)\left(\sum_{n=0}^{\infty}\sqrt{n}\,\Psi_{n-1}^{*}\Psi_n\right)+\mathbf{\Phi}^{*}(\mathbf{r},t)\left(\sum_{n=0}^{\infty}\sqrt{n}\,\Psi_{n-1}\Psi_n^{*}\right).$$

In this expression, the function

$$\mathbf{\Phi}(\mathbf{r},t)=\frac{\mathrm{i}\sqrt{\hbar}}{2\pi}\sum_{\lambda}\int \mathrm{d}\mathbf{k}\ \sqrt{\omega}\,W_{\lambda}^{*}(\mathbf{k})\,\mathbf{e}_{\lambda}(\mathbf{k})\exp\left[\mathrm{i}(\mathbf{kr}-ckt)\right] \tag{2.8}$$

is the above function describing the shape of the wave packet.

The mean square of the field strength, proportional to the electric energy density, is expressed via the same wave packet shape:

$$\left\langle\mathbf{E}^2(\mathbf{r},t)\right\rangle=\left|\mathbf{\Phi}(\mathbf{r},t)\right|^2\left(\sum_{n=0}^{\infty}n|\Psi_n|^2\right).$$

It can be shown that the average values of all field strength powers are expressed through function (2.8).

Consequently, function $\mathbf{\Phi}(\mathbf{r},t)$ describes the field distribution in any quantum state of the field. For this reason, a photon in the packet representation is a spatially localized object. For a one-photon state, function $\mathbf{\Phi}(\mathbf{r},t)$ can be referred to as the photon shape. In the case of a multiphoton state, however, there is no spatial separation of the packet into particular one-photon parts: the fields of all the photons are uniformly distributed in accordance with the function $\mathbf{\Phi}(\mathbf{r},t)$.

It follows from relation (2.8) that the quantity

$$\frac{\mathrm{i}\sqrt{\hbar\omega}}{2\pi}\,W_{\lambda}^{*}(\mathbf{k})$$

is just the Fourier spectrum of the wave packet $\mathbf{\Phi}(\mathbf{r},t)$. It is known that the length $L$ of the packet and the width $\Delta\omega$ of its spectrum obey the condition

$$\Delta\omega\,\frac{L}{c}\geqslant 1\,.$$

Consequently, the photon length $L_{\text{phot}}=L$ can only be larger than the characteristic packet length equal to the coherence length and defined by the relation

$$L_{\text{coh}}=\frac{c}{\Delta\omega}\,,\quad\text{i.e.,}\quad L_{\text{phot}}\geqslant L_{\text{coh}}=\frac{c}{\Delta\omega}\,.$$

Applying this relation to photons generated in highly coherent lasers, it can be inferred that, at coherence times of order one second, the photons have an astronomic length on the order of the distance between the Earth and the Moon. Evidently, such photons cannot be the cause of photocounts.

Such is the view of photon localization in the context of QED. It is sometimes assumed that radiation, even a coherent one, contains some localized objects that are not described by the QED mathematical apparatus and that it is these objects that should be called photons. We think that this opinion is naive. Quantum electrodynamics has a history of more than half a century, and it is fairly well verified experimentally. It seems very unlikely that such a theory could overlook certain localized objects.

### 2.3 The photoeffect and electron localization

Let us now consider two other opinions according to which the discreteness of the detector output signal originates from

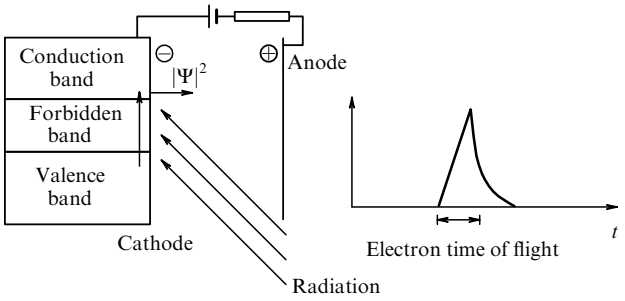


**Figure 2.** How is the electron wave leaving the cathode transformed to a particle?

the discreteness of the electron itself. The layout of a vacuum [1] radiation detector is presented in Fig. 2.

**2.3.1 Photoeffect.** According to the photoeffect theory, a plane electromagnetic wave interacts with a plane Bloch electron wave of the valence band in the semiconductor making up the cathode. The interaction results in a Bloch electron wave in the conduction band. Its energy being much higher than that of the wave in the valence band, this wave easily penetrates into the vacuum, surmounting the potential barrier. In other words, the electron is regarded up to this moment as a wave having no internal spatial localization. [2] Excitation of the electron wave in the conduction band under the influence of a continuous electromagnetic wave proceeds continuously; hence, there is no indication of the possibility of discrete output signals at this stage.

If the description of the electron wave (specifically as a wave) is extended as far as the anode, there will be no current splashes, i.e., photocounts because, on the one hand, a continuous wave cannot produce any splash in the current, and, on the other hand, photocounts are known to appear just as the electron flies across the cathode – anode gap. Hence, if photocounts did not occur before the wave reached the anode, they will never occur at all. Certainly, such a description is in conflict with observations, since the existence of photocounts is a well-established experimental fact.

**2.3.2 Wave packet reduction.** An electron wave leaving the cathode for the vacuum is usually understood as the probability amplitude of the discovery of a localized electron in the vicinity of the cathode. Such an interpretation is supported by the reference to the 'wave packet reduction' that takes place in quantum-mechanical measurements, i.e., during the interaction between the microscopic quantum system and a macroscopic instrument. Because the electron becomes a randomly localized particle, the photocount arises naturally as the particle moves across the gap between the cathode and the anode.

However, such an application of the 'wave packet reduction' concept is irrelevant. Putting aside all ongoing debates on wave packet reduction, we refer to the opinion of such a reputable author as von Neumann [10]. He justly argues that the notion of wave packet reduction is applicable only when the imaginary surface separating the quantum system from the device can be transferred as a whole by including the device or its parts in the quantum system. In so doing, the picture perceived by the observer must remain unaltered because the surface separating the quantum system from the device is an imaginary one and therefore cannot produce any effect. Von Neumann made many efforts to demonstrate that such measurements are possible.

However, this is not the case considered in the proposed explanations of photocounts, which are based on the wave packet reduction concept. As mentioned above, a shift in the boundary between a system regarded as a quantum-mechanical one and a 'classical' device from the cathode to the anode substantially changes the picture observed — that is, photocounts disappear. Therefore, the wave packet reduction, if any, occurs at a later stage of the interaction between the quantum system and the instrument.

To summarize, it should be recognized that the current concepts of optical signal detection do not explain photocounts, i.e., discrete responses of a photodetector to a continuous signal being received.

### 2.4 The photocounts as a manifestation of the Coulomb instability of a low electron flux

The above line of reasoning leads to the conclusion that photocounts need a physical explanation other than a mysterious transformation of a wave to a particle. It is assumed in this review that the cause of photocounts is the Coulomb instability of a low electron flux in the photodetector, induced by the received radiation [6]. This instability facilitates the breakdown of the flux into separate one-electron bunches that travel from the cathode to the anode and induce splashes in the electric current in the external circuit of the detector. The observer perceives these splashes as photocounts.

**2.4.1 Wigner instability.** The instability of a low electron flux is easy to understand in the context of the well-known Wigner crystallization [7]. It is common knowledge that a low-density system of electrons breaks down into systematically positioned one-electron bunches that Wigner called electrons. Two stages are distinguished in this crystallization. One is the instability of the uniform or quasi-uniform electron distribution (referred to as Wigner instability) and the onset of breakdown into bunches. The other is the Wigner crystallization proper or self-organization of the electron distribution under the steady-state Wigner conditions.

Electromagnetic radiation that reaches a vacuum detector makes electrons transfer from the high charge density zone inside the cathode to the low charge density zone in the vacuum. Accordingly, this gives rise to a tendency toward the breakdown of the quasi-uniform electron distribution into bunches. However, the final stage, i.e., regular crystallization, is not reached on the whole, hampered by nonstationary conditions in the detector. The breakdown results only into more or less chaotic bunches. [3]

It is these bunches travelling between the cathode and the anode that excite chaotic splashes in the current in the

[1] Instabilities similar to those considered below must be manifested in semiconductor detectors as well. However, their theoretical consideration is very difficult because of the presence of the medium.

[2] It is worthwhile to note that all the main laws governing the photoelectric effect (*inter alia* the law that predicts the photoelectric threshold) are realized at this preliminary stage of the interaction between the wave and the photocathode. For this reason, the concept of photocounts being developed below by no means interferes with these manifestations; in fact, it supplements them.

[3] It should be noted, however, that self-organization is possible under certain special conditions in the electron flux [13].

external circuit of the detector, being interpreted by the observer as photocounts. This explanation of photocounts proposed in our papers [6, 11] is currently the only one free from serious controversy. Arguments in favor of this opinion are presented below.

**2.4.2 Breakdown of an electron cloud into bunches.** In order to illustrate the breakdown of an electron cloud into bunches at small electron densities, we considered a system of two-electrons located in a quadratic potential well and interacting with each other in conformity with the Coulomb law [12]. Then, the potential energy of the system is given by

$$U(\mathbf{r}_1, \mathbf{r}_2) = \beta(\mathbf{r}_1^2 + \mathbf{r}_2^2) + \frac{e^2}{|\mathbf{r}_1 - \mathbf{r}_2|},$$

where $\mathbf{r}_1$, $\mathbf{r}_2$ are radius vectors of the first and second electrons, and $\beta$ is the potential well parameter, the growth of which is accompanied by the narrowing of the potential well. The stationary wave functions of the system and the corresponding energies were calculated by the basis-free variational method [4, 5, 12]. The results are presented in Figs 3 and 4. Figure 3 shows the dependence of the energy of the two-electron cloud on the width of the potential well. The electron cloud may reside in two states, either with one (curve *1*) or two (curve *2*) charge density maxima. In a wide potential well, the energetically most preferable state is that with two maxima, while in a narrow potential well that with one maximum. Thus, it is possible to control the electron density of the system under consideration by varying the parameter of the potential well and to determine the point in time at which the electron cloud begins to break down into one-electron bunches. As the electron density decreases, the cloud breaks down into two electrons. This confirms Wigner's inference for the specific conditions of a potential well.

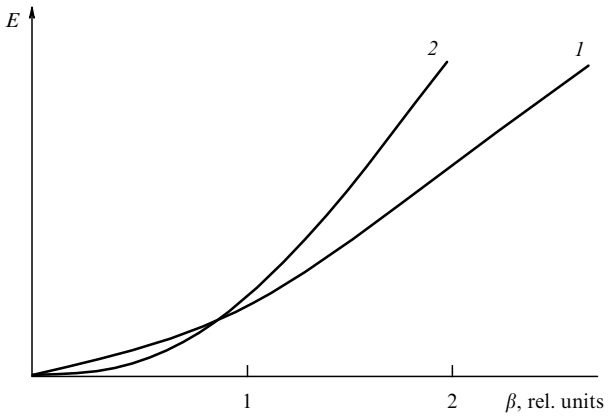


**Figure 3.** Energies of symmetric and asymmetric states plotted as a function of the parameter of a quadratic potential well, which is inversely proportional to the well width.

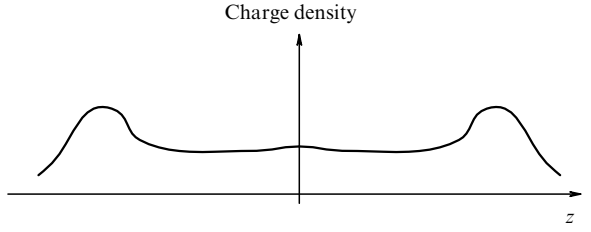


**Figure 4.** Breakdown of an electron cloud into two bunches in a quadratic potential well.

It is understandable that such a breakdown into one-electron bunches must occur when a low-density electron wave escapes the cathode and enters the vacuum. However, Fig. 4 based on the results of calculations shows that such one-electron bunches are rather smeared-out entities which are unlikely to produce sharp current pulses resembling photocounts in the external circuit of a photodetector. This implies another mechanism responsible for the sharpening of these bunches.

**2.4.3 Mechanism of sharpening of electron bunches.** The Coulomb field is possessed of a focusing ability, although this property is not obvious. In order to demonstrate it in the framework of the classical (nonquantum) picture, we considered two examples of the expansion of charged particle packets: the radial expansion of a spherically symmetric Gaussian packet, and the expansion of a cylindrical Gaussian packet distributed along the cylinder axis [6]. It was shown that such an expansion results in charge density maxima referred to as catastrophes in the mathematical literature [14]. Monastyrskii [15] also considered a temporal progress of the overtaking-type catastrophe resulting from the Coulomb repulsion in a many-electron packet travelling in an electron image tube designed to record picosecond laser pulses.

**2.4.4 Expansion of the spherically symmetric Gaussian charge distribution.** The spherically symmetric case is convenient in that the equation of motion of the charged packet layers is integrated over a time interval from the beginning of motion to the onset of overtaking. Due to this, the formation of electron density maxima can be investigated analytically. Details of the computation are presented in Appendix 1. Figure 5 illustrates how the initial Gaussian distribution of charge density varies with time under the action of its own

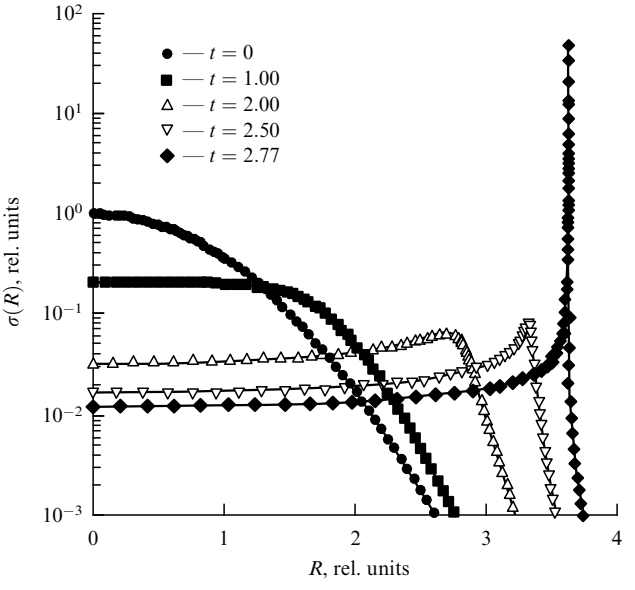


**Figure 5.** Formation of the electron density maximum as the bunch breaks down under the action of the electric field of its own charge. $\sigma(R)$ — charge density, and $R$ — layer radius; time $t$ is given in relative units.

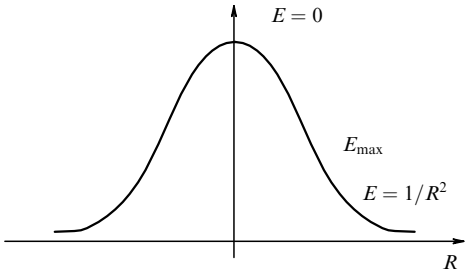


**Figure 6.** Layers at the charge distribution slope leave behind the peripheral layers, giving rise to a charge density maximum.

Coulomb field. It can be seen that at a certain instant of time the cloud exhibits, at first sight without any apparent cause, an infinite charge density maximum. This means that the electric field of a localized charge possesses some focusing properties. The physical explanation of this observation is simple and can be understood from Fig. 6. The electrical field in the center vanishes by virtue of the charge distribution symmetry. It is also small at the periphery of the charge distribution, in accordance with the Coulomb law. Hence, there is a field maximum on the charge distribution slope. The charge distribution layers on the slope accelerate and begin to leave behind the peripheral layers, giving rise to the maximum (catastrophe) on the distribution slope. The sharp peak in Fig. 5 has an infinite amplitude. However, this maximum is finite, even if large, taking into consideration the wave nature of the electron. It can be assumed that such a focusing promotes sharpening of the somewhat smeared-out electron bunches formed as a result of the Wigner instability. Further computation in the framework of quantum mechanics actually confirmed this inference (see Section 2.4.6).

**2.4.5 Expansion of a charged bunch distributed along the axis according to the Gaussian law.** Only the results of computations are presented here, as in the spherical case (see papers [6] for detailed discussion). The picture in Fig. 7 resembles the spherically symmetric case in that an electron density maximum develops with time. However, it is possible to observe the dependence on the transverse distribution size. It can be seen that the smaller the distribution diameter (i.e., the higher the charge density), the earlier the inhomogeneities are formed. From this follows an important conclusion. With the electron packet travelling between the electrodes in the focusing static field of a vacuum device, with high probability the maximum compression of the electron bunch in the longitudinal and traverse directions occurs almost simultaneously. This, in turn, further promotes sharpening of the pulse induced by the electron bunch in the external circuit of the detector.

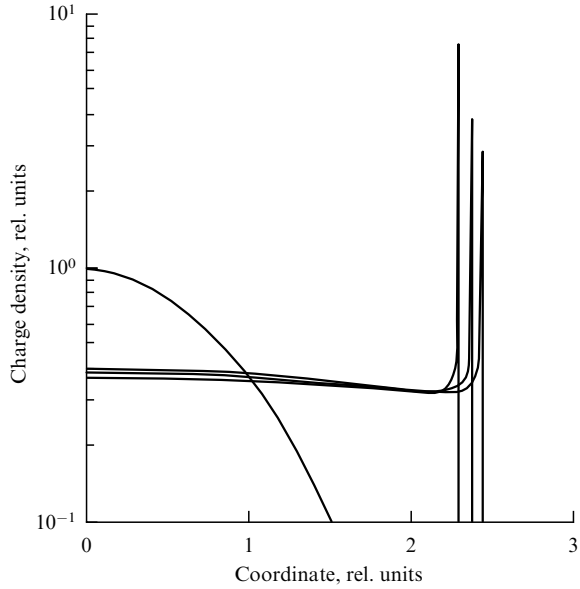


**Figure 7.** Formation of a charge density maximum in the case of linear charge distribution.

**2.4.6 Longitudinal compression of a one-electron bunch as it moves in the cathode – anode field and at the same time in the Coulomb field of another similar bunch (quantum-mechanical problem).** Many quantum-mechanical problems pertaining to the motion of wave packets in smoothly varying fields of different configurations can be resolved by our method developed in Ref. [16] (see also Appendix 2). In this method, the wave packet is regarded as a Gaussian one:

$$\Psi(\mathbf{r},t) = C(t)\exp\left\{-(\boldsymbol{\rho},F\boldsymbol{\rho}) + \frac{\mathrm{i}}{\hbar}\left[\left(\mathbf{p}_0(t),\boldsymbol{\rho}\right) + E(t)\right]\right\}. \quad (2.9)$$

Here, $\boldsymbol{\rho} = \mathbf{r} - \mathbf{r}_0(t)$ and quantities $\mathbf{r}_0(t)$ and $\mathbf{p}_0(t)$ obey the classical Hamilton equations

$$\frac{\mathrm{d}\mathbf{r}_0}{\mathrm{d}t} = \frac{\mathbf{p}_0}{m_\mathrm{e}}\,, \qquad \frac{\mathrm{d}\mathbf{p}_0}{\mathrm{d}t} = -\mathrm{grad}\,U(\mathbf{r}_0)\,, \quad (2.10)$$

where $U(\mathbf{r})$ is the potential in which the wave packet is travelling. The real part of the complex matrix $F(t)$ determines the spatial distribution of the wave function module, while its imaginary part defines that of the wave function phase. It is shown in Appendix 2 that a change in matrix $F(t)$ with time is described by a nonlinear matrix equation of the Riccati type

$$\mathrm{i}\hbar\,\frac{\mathrm{d}F}{\mathrm{d}t} = \frac{2\hbar^2}{m_\mathrm{e}}\,F^2 - \frac{1}{2}\,U''\,, \quad (2.11)$$

where $U''$ is the matrix of the second derivatives of the potential energy in the center of the wave packet that emerges upon the expansion of the potential energy in a Taylor series in the vicinity of the packet center:

$$U(\mathbf{r}_0+\boldsymbol{\rho}) = U(\mathbf{r}_0) + \left(\boldsymbol{\rho},\mathrm{grad}\,U(\mathbf{r}_0)\right) + \frac{1}{2}(\boldsymbol{\rho},U''\boldsymbol{\rho}) + \ldots\,. \quad (2.12)$$

This method is suitable provided it is possible to neglect the terms with cubic and higher degrees of smallness in potential (2.12). It has been shown in Ref. [16] that nonlinear equation (2.11) is reduced to a system of linear equations and in many cases can be solved with relative ease. It follows from Eqn (2.11) that the dynamics of the packet parameters responsible for its dimensions is determined by the matrix of the second derivatives of the field potential with respect to the spatial coordinates at a point corresponding to the packet center.

This method was applied to follow the passage of an electron bunch across the interelectrode space. In the one-dimensional case and a uniform cathode – anode field

($U'' = 0$), it is possible to integrate Eqn (2.11). Assuming the parameter $F_0$ to be purely real at the initial point in time, it is easy to obtain the time dependence of the longitudinal packet half-width:

$$a_1 = a_0\sqrt{1 + \frac{t^2}{\tau^2}}\,, \tag{2.13}$$

where $\tau = ma_0^2/\hbar$ is the characteristic packet expansion time, and $a_0$ is the initial packet half-width. The time of flight of an electron between the cathode and the anode is on the order of

$$t_0 = \sqrt{\frac{2ml}{eU}}\,, \tag{2.14}$$

where $l$ is the distance between the cathode and the anode and $U$ is the voltage between them. Parameters $\tau$ and $t_0$ must be of the same order to prevent substantial expansion of the electron packet as it travels from the cathode to the anode. The characteristic size of the packet also exists, so that

$$A = \sqrt[4]{\frac{2\hbar^2 l^2}{eUm}}\,. \tag{2.15}$$

If the packet were much smaller than the characteristic size (2.15), it would rapidly and diffusely spread out and produce no sharp current splash (i.e., a photocount) in the external circuit of the detector. Therefore, it may be concluded that the dimension of real packets in vacuum devices is on the order of the characteristic size. Note also that the characteristic size $A$ exhibits only weak dependence on the parameters $U$ and $l$ of the device.

The distance between the cathode and the anode is usually about 1 cm, and the voltage is approximately 100 V. Hence, according to formula (2.15), one obtains

$$A = 6 \times 10^{-5}\ \text{cm}\,. \tag{2.16}$$

Thus, the characteristic size is rather large, around 1 μm. Accordingly, the dimensions of the wave packet in a vacuum photodetector must be greater (or even much greater) than the characteristic size $A$, if it is to undergo no substantial change during the motion from the cathode to the anode. Moreover, the packet dimensions must be limited from above — that is, they must be significantly smaller than the characteristic distance between the cathode and the anode to enable a sharp current pulse to be generated in the external circuit of the photodetector.

In real conditions, electron wave packets travel not only in the cathode–anode field but in each other's Coulomb fields as well. This situation was also considered using the above approach. However, equation (2.11) can be solved in this case only numerically. Figure 8 displays the dependence of the width of a one-electron bunch on the traversed distance during its motion in the cathode–anode field and at the same time in the field of another similar bunch. It can be seen that the nonuniform field of the second electron bunch strongly focuses the travelling bunch, so that its longitudinal size decreases by several orders of magnitude. Such an electron bunch can induce a sharp splash in the current resembling a photocount in the external circuit of the photodetector.

To sum up, the Coulomb instability of the quasi-uniform electron distribution is deemed to account for the physical picture of photocounts observed during the detection of weak optical signals. At present, this appears to be the sole noncontradictory explanation for the main features of this picture.

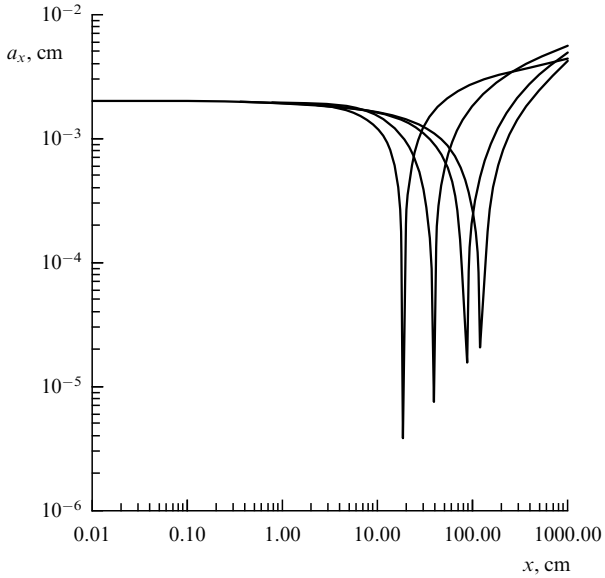


**Figure 8.** Compression of an electron bunch travelling in the cathode–anode field and simultaneously in the field of another charge: $a_x$ — length of the electron bunch, and $x$ — distance covered by the bunch.

## 2.5 The possibilities of experimental examination of one-electron bunches in vacuum devices

**2.5.1 Scattering of pulsed laser radiation by an electron wave packet.** Because the dimensions of an electron packet are comparable to typical optical wavelengths, the natural way to observe the packet is its probing by an intense laser pulse and detecting radiation scattered from it. Let us, therefore, assume that in the path between the cathode and the anode an electron packet flies across an intense pulsed laser beam.

In order to estimate the scattered energy, we shall consider the case where the packet dimensions are significantly smaller than the lasing wavelength. Then, the intensity of the scattered radiation (Thomson scattering) is determined in the dipole approximation as [17]

$$I = \frac{2e^2a^2}{3c^3}\,, \tag{2.17}$$

where the acceleration of the packet is

$$a = \frac{eE(t)}{m}\,, \tag{2.18}$$

and $E(t)$ is the strength of the laser radiation field. This strength is related to the laser pulse energy $W$ by the expression

$$E^2 = \frac{4\pi W}{c\tau S}\,, \tag{2.19}$$

where $\tau$ is the pulse duration, and $S$ is the cross section of the beam at the site where it is intersected by the electron packet. The number of photons scattered by the electron packet equals

$$N = \frac{\tau I}{\hbar\omega} = \frac{4\varepsilon^2\hbar\lambda W}{3m^2c^3S}\,, \tag{2.20}$$

where $\varepsilon = e^2/\hbar c$ is the fine-structure constant ($\varepsilon \approx 1/137$), and $\lambda$ is the lasing wavelength.

It is known that at the present time the intensity of focused laser radiation can be as high as $I_0 \approx 10^{21}$ W cm$^{-2}$ at a pulse duration of about $10^{-12}$ s, i.e., $W/S = \tau I_0 \approx 10^{16}$ erg cm$^{-2}$. The estimation using formula (2.20) indicates that a single electron wave packet scatters $N \approx 4 \times 10^3$ photons. This number being rather high, the scattered radiation can be a sensitive indicator of the presence of the electron wave packet. When the dimensions of the packet are smaller than the laser wavelength, the angular distribution of the scattered radiation shows dipole behavior. As the wavelength decreases, the angular distribution of the scattered radiation progressively deviates from the dipole distribution, and the difference contains information about the dimensions and shape of the electron packet. Specifically, the smaller the laser wavelength, the greater the difference between the scattering intensities along the laser beam and perpendicular to it.

**2.5.2 Deflection of an electron wave packet from the rectilinear trajectory by a laser pulse.** Let us consider the radiation pressure exerted by a laser pulse on the electron packet. Photons being equally scattered by the electron packet in the forward and backward directions along a laser beam, it may be assumed that their motion is on the average arrested and they give their momenta to the electron packet. Because each photon transfers a momentum $\hbar\omega/c$, the velocity component of the electron packet, parallel to the laser beam, is equal after interacting with it to

$$V = \frac{N\hbar\omega}{mc} = \frac{8\pi\alpha^2\hbar^2 W}{3m^3c^3S} \,. \tag{2.21}$$

The substitution of the $W/S$ ratio from Section 2.5.1 into formula (2.21) yields

$$V \approx 3 \times 10^8 \text{ cm s}^{-1} \,. \tag{2.22}$$

In other words, the velocity component of the electron packet along the laser beam is comparable with its initial velocity. This means that the electron packet is deflected from its original direction through an angle of several radians. This deflection, similar to the scattered light, can be an indicator of the packet passage through the detector. As the wavelength of the laser radiation decreases and becomes comparable to or smaller than the packet dimensions, photons are increasingly scattered forward and the deflection of the electron packet also decreases. This decrease may serve as a measure of the packet dimension.

**2.5.3 Electrostatic defocusing of one-electron wave packets.** Let us consider the motion of an electron wave packet towards the center of a macroscopic spherical electrode with a negative potential (Fig. 9). The wave packet, having a sufficiently high initial velocity, stops near the spherical electrode and remains a relatively long time in the strong nonuniform electrostatic field that defocuses it in the transverse direction. Notice that in the vicinity of the point where the center of the packet came to rest, the dependence of its potential energy on the longitudinal and transverse coordinates has the form of a saddle: the focusing, roughly quadratic potential in the longitudinal direction, and the defocusing, also approximately quadratic potential in the transverse direction. Such

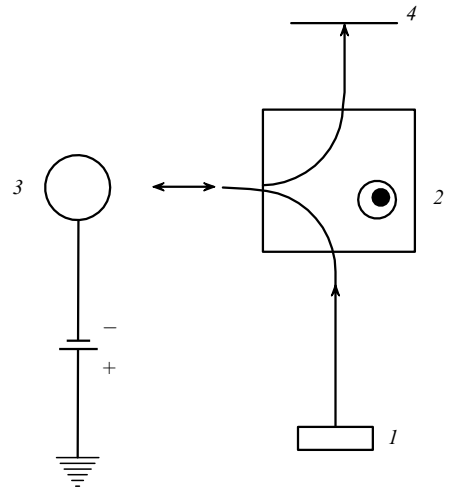


**Figure 9.** Enlargement of the transverse dimensions of an electron bunch travelling in a defocusing field: *1* — source of electrons, *2* — magnetic field region directing the electrons toward the defocusing electrode, *3* — defocusing electrode, and *4* — screen.

a behavior of the potential energy in the vicinity of the stop-point of the electron packet center determines its subsequent dynamics.

Calculations revealed [18] that in the case under consideration, the initially microscopic wave packet turns into an essentially macroscopic one; upon scattering by the potential of the sphere, the transverse dimensions of the packet rather rapidly, on a half-meter trajectory, approach about 1 cm.

It is worthwhile to mention a now well-established fact, namely the possibility for electrons to be in a state with a wave packet of macroscopic dimensions. An example is provided by the so-called Rydberg atoms, i.e., strongly excited atoms with a large principal quantum number. As demonstrated by means of space radiospectroscopy, atoms in the rarefied interstellar medium may reside in states with a large principal quantum number, when the linear dimensions of the electron cloud are as large as a few millimetres. The Rydberg atoms obtained under laboratory conditions have a diameter of about 0.01 mm that is greater than the diameter of a ground-state atom by a factor of $10^5$.

Experiments designed to substantially widen electron wave packets might be of primary importance. For example, it is impossible to say in advance whether a wide wave packet ($\approx$ 1 cm) can cause luminescence of the entire screen area it covers or only a small point on it; it should be recalled that the energy of the packet is sufficient to emit $\approx$ 1000 photons.

## 3. Reception of signals without photocounts. Laser detection

The main conclusion that follows from the studies on the nature of photocounts, the results of which were presented in Section 2, is that photocounts are no absolute phenomenon unamenable to any effect. Photocounts result from a certain type of instability of an electron flux, specifically the Coulomb instability. This means that this phenomenon can be avoided by stabilizing the electron system of the photodetector through one method or another. This is an important conclusion because the absence of photocounts is associated with markedly depressed shot noise in the detector.

### 3.1 Laser detection. Principle of action

The problem of detecting optical signals by allied optical means appears to have been first formulated by Bloembergen [19]. However, this idea had no further serious development. The sensitivity of schemes for the direct amplification of optical signals propagating through an amplifying medium is significantly restricted by noises associated with the intrinsic spontaneous emission of this medium [20]. It was shown in Ref. [21] that the signal-to-noise ratio can be improved by applying nonlinear radiation detectors in which the transformation of the signal begins from an absorptive transition.

As shown in Section 2, conventional radiation detectors are characterized by a strong Coulomb instability of the low electron flux induced by the signal being detected. This instability is due to the use of free electrons in such devices. In other words, their electron system is strongly degenerate. It is well known that strongly degenerate systems easily rearrange themselves under the action of external factors because the process requires only small energy expenditure. The degeneracy of the electron system in such detectors is responsible for the breakdown of a low electron flux into bunches under the effect of the exciting Coulomb interaction. This prompts the employment of electrons bound in atoms, ions, or molecules in such devices instead of free electrons, because they are fairly well stabilized there by strong nuclear Coulomb fields. This makes impossible any instability associated with the collective motion of bound electrons in atomic and molecular particles.

In what follows, we describe a possible scheme for the detection of weak optical signals using bound electrons [22]. It is proposed to call this method laser detection because it extensively utilizes laser radiation.

The basic component of the scheme is a system of three-level atoms (Fig. 10). It is assumed that the atoms are confined in a specially constructed optical resonator having the resonance, signal mode at frequency $\omega$ of the $|0\rangle \leftrightarrow |1\rangle$ transition and two resonance modes at frequency $\Omega$ of the $|1\rangle \leftrightarrow |2\rangle$ transition. In the absence of populations at levels $|1\rangle$ and $|2\rangle$, the last two modes are degenerate in frequency and not coupled to each other (they may differ, for example, in polarization and have virtually identical spatial distribution). In this case, one of them (the pump mode) is excited, i.e., contains a strong monochromatic pump field established by an external source. The other mode, hereinafter referred to as the output mode, is intended to excite the output signal. In the initial state, i.e., before the arrival of the signal, the output mode is not excited and contains no field.

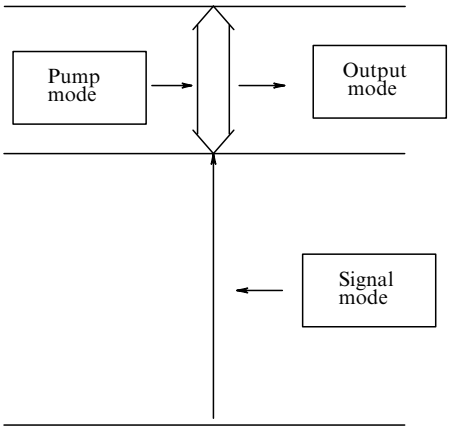


**Figure 10.** Interaction of a three-level system with optical modes during laser detection of optical signals.

The principle of action of the detector is as follows. Before the arrival of a signal in the signal mode, the atom is out of resonance with the pump field and does not practically interact with it, remaining in the state $|0\rangle$. The arrival of a signal at frequency $\omega$ brings about some population to the level $|1\rangle$, and the strong pump field induces transitions between levels $|1\rangle$ and $|2\rangle$. This results in an oscillating dipole moment at frequency $\Omega$ that excites the field in the output mode. The problem is to demonstrate that the output signal can be substantially stronger than the input one. Moreover, it is necessary to determine the characteristic building-up time of the output signal. The study is carried out in the so-called semiclassical approximation in which intraatomic processes are considered in the framework of quantum mechanics, whereas all fields are taken to be classical.

It is worthwhile to emphasize a similarity between laser and traditional methods employed to detect optical signals. In either case, an electron becomes excited after the arrival of the signal to be detected and obtains access to the source of energy. In a conventional photodetector, such a source is represented by the constant cathode–anode field; in the case of laser detection, the intense laser field serves as the energy source. The signal being detected in both situations undergoes frequency transformation. The characteristic frequency at the output of the traditional detector is on the order of $10^8$ Hz. Whereas in laser detection, the characteristic output frequency differs from the frequency of the signal being detected but falls within the same optical range.

### 3.2 Small time of the detector response to an external signal in the absence of relaxation

Let us first consider a case where the building-up time of the output signal is smaller than the phase (transverse) relaxation time of active atoms in the medium.

The state of a three-level atom is subject to change under the action of three fields: the signal field, the pump field, and the originally unknown field of the output mode. The field of the output mode is excited by the polarization current of the atomic system. Taking into consideration the evolution of the atoms and the excitation of the output mode leads to a self-consistent problem, the solution of which permits us to find the field in the output resonant cavity and determine the building-up time of the output signal.

**3.2.1 Excitation of a cavity field by external current.** Cavity fields in the Coulomb gauge are described by the equations

$$\Delta \mathbf{A} - \frac{1}{c^2}\frac{\partial^2 \mathbf{A}}{\partial t^2} = -\frac{4\pi}{c}\,\mathbf{j}_c\,, \qquad \operatorname{div}\operatorname{grad} U = -4\pi\rho\,, \tag{3.1}$$

where the eddy current is given by

$$\mathbf{j}_c = \mathbf{j} - \frac{1}{4\pi}\operatorname{grad}\frac{\partial U}{\partial t}\,.$$

The resonant cavity contains a set of modes $\mathbf{v}(\mathbf{r})$ obeying equations

$$\Delta \mathbf{v} + k^2 \mathbf{v} = 0\,, \qquad \operatorname{div} \mathbf{v} = 0\,,$$

necessary boundary conditions and being orthonormalized in the following way:

$$\int \mathrm{d}\mathbf{r}\ \mathbf{v}_k(\mathbf{r})\,\mathbf{v}_l(\mathbf{r}) = \delta_{kl}\,.$$

The first of equations (3.1) is multiplied by the distribution $\mathbf{v}_\mathrm{o}(\mathbf{r})$ corresponding to the output mode[4] and integrated over the cavity volume. Further integration by parts yields

$$\ddot{U}(t) + \Omega^2 U(t) = 4\pi c j(t)\,,$$

where

$$U(t) = \int \mathrm{d}\mathbf{r}\ \mathbf{v}_\mathrm{o}(\mathbf{r})\,\mathbf{A}(\mathbf{r},t)\,, \qquad j(t) = \int \mathrm{d}\mathbf{r}\ \mathbf{v}_\mathrm{o}(\mathbf{r})\,\mathbf{j}_\mathrm{c}(\mathbf{r},t)\,, \quad (3.2)$$

and $\Omega$ is the mode eigenfrequency. It can be shown that the part of the integral $j(t)$ containing grad $U(\mathbf{r})$ equals zero. Therefore, it is possible to use the total current instead of the eddy current in the definition of $j(t)$.

Furthermore, the field amplitude $U(t)$ is assumed to be a slowly varying function of time in which a negative-frequency part is distinguished:

$$U^{(-)}(t) = u(t)\exp(-\mathrm{i}\Omega t)\,.$$

Then, neglecting the second derivative of the amplitude $u(t)$ with respect to time, the equation of excitation of the output mode takes the form

$$u(t) = \frac{2\pi\mathrm{i}c}{\Omega}\,j'(t)\,, \quad (3.3)$$

where $j'(t)$ is the amplitude of the negative-frequency part of the current $j(t)$:

$$j^{(-)}(t) = j'(t)\exp(-\mathrm{i}\Omega t)\,,$$

which is also considered to be a slowly varying function of time.

Thus, the field amplitude in the output mode can be found knowing the current that excites this mode; it is constituted by the elementary currents of individual atoms interacting with the three fields.

**3.2.2 Dynamics of active atoms under the effect of three fields.** Because we are going to take into account phase (or transverse) relaxation in what follows, the state of the three-level atoms interacting with the fields of the three modes will be described by the density matrix

$$\begin{aligned}\rho = {} & \rho_0|0\rangle\langle 0| + \rho_{01}|0\rangle\langle 1| + \rho_{02}|0\rangle\langle 2| \\ & + \rho_{10}|1\rangle\langle 0| + \rho_1|1\rangle\langle 1| + \rho_{12}|1\rangle\langle 2| \\ & + \rho_{20}|2\rangle\langle 0| + \rho_{21}|2\rangle\langle 1| + \rho_2|2\rangle\langle 2|\,. \end{aligned} \quad (3.4)$$

The evolution of a three-level atom interacting with the fields of the three modes is governed by the Hamiltonian

$$H(t) = H_0 + V(t)\,, \quad (3.5)$$

[4] Hereinafter, indices o (out) and i (in) refer to the output and the signal modes, respectively; quantities referring to the pump mode have no index.

where

$$H_0 = \hbar\omega|1\rangle\langle 1| + \hbar(\omega+\Omega)|2\rangle\langle 2|\,, \quad (3.6)$$

$$\begin{aligned} W(t) = \frac{V(t)}{\hbar} = {} & \left[\alpha|2\rangle\langle 1|\exp(-\mathrm{i}\Omega_0 t) + \alpha^*|1\rangle\langle 2|\exp(\mathrm{i}\Omega_0 t)\right] \\ & + \left[\gamma(t)|2\rangle\langle 1|\exp(-\mathrm{i}\Omega t) + \gamma^*(t)|1\rangle\langle 2|\exp(\mathrm{i}\Omega t)\right] \\ & + \left[\beta|1\rangle\langle 0|\exp(-\mathrm{i}\omega_0 t) + \beta^*|0\rangle\langle 1|\exp(\mathrm{i}\omega_0 t)\right]\,, \end{aligned} \quad (3.7)$$

and $\Omega_0$ and $\omega_0$ are the frequencies of the pump and the signal, respectively (considered below is the resonance case when $\Omega_0 = \Omega$, and $\omega_0 = \omega$).

The first and the second terms in $V(t)$ describe the interactions of the atom with the pump and output modes, respectively. The third term in $V(t)$ describes the interaction between the atom and the signal field to be detected at frequency $\omega_0$ equalling the resonant frequency $\omega$ of the $|0\rangle \to |1\rangle$ transition. Because the field amplitude of the output mode, proportional to $\gamma(t)$, slowly varies with time, this field is not monochromatic. Its average frequency is fixed at a level of $\Omega$.

In the interaction representation, the density matrix obeys the equation

$$\frac{\partial\rho}{\partial t} = -\mathrm{i}[W_\mathrm{i};\rho]\,, \quad (3.8)$$

where

$$\begin{aligned} W_\mathrm{i}(t) &= \exp\left(\frac{\mathrm{i}H_0 t}{\hbar}\right) W(t)\exp\left(-\frac{\mathrm{i}H_0 t}{\hbar}\right) \\ &= \left[\zeta(t)|2\rangle\langle 1| + \zeta^*(t)|1\rangle\langle 2|\right] + \left[\beta|1\rangle\langle 0| + \beta^*|0\rangle\langle 1|\right]; \end{aligned} \quad (3.9)$$

$$\begin{aligned} &\zeta(t) = \alpha + \gamma(t)\,, \qquad \alpha = -\frac{\mathrm{i}e\Omega u r}{\hbar c}\,, \\ &\beta = -\frac{\mathrm{i}e\omega u_\mathrm{i} r_\mathrm{i}}{\hbar c}\,, \qquad \gamma(t) = -\frac{\mathrm{i}e\Omega u_\mathrm{o}(t) r_\mathrm{o}}{\hbar c} \end{aligned} \quad (3.10)$$

are the quantities that describe the interaction between the atom and the field modes; $u$, $u_\mathrm{i}$, and $u_\mathrm{o}(t)$ are the negative-frequency amplitudes of the vector potential of the pump, signal, and output modes, respectively, and

$$r = \mathbf{v}(0)\,\mathbf{r}_{21}\,, \qquad r_\mathrm{i} = \mathbf{v}_\mathrm{i}(0)\,\mathbf{r}_{10}\,, \qquad r_\mathrm{o} = \mathbf{v}_\mathrm{o}(0)\,\mathbf{r}_{21} \quad (3.11)$$

are the projections of matrix elements of the electron coordinate $\mathbf{r}$ on the amplitudes $\mathbf{v}$, $\mathbf{v}_\mathrm{i}$, and $\mathbf{v}_\mathrm{o}$ of the normalized pump, signal, and output modes at the point of atomic location, i.e., at the origin of the coordinates (where due to mode normalization one finds $\mathbf{v}^2 \approx 1/V$, where $V$ is the mode volume).

The atomic current density operator is defined in the following way:

$$\mathbf{J}(\mathbf{r},\mathbf{q}) = \frac{e}{m}\,\mathbf{p}\,\delta(\mathbf{r}-\mathbf{q})\,.$$

For the current responsible for the transition $|1\rangle \leftrightarrow |2\rangle$ in the interaction representation, the following equation holds:

$$\mathbf{j}(\mathbf{r},t) = \frac{e}{m}\left(\langle 2|\mathbf{p}\,\delta(\mathbf{r}-\mathbf{q})|1\rangle\right)\exp(\mathrm{i}\Omega t)|2\rangle\langle 1| + \text{H.c.}$$

In the dipole approximation, the polarization current $j(t)$ exciting the output mode assumes the form

$$\begin{aligned} j(t) &= n\int \mathrm{d}\mathbf{r}\ \mathbf{v}_\mathrm{o}(\mathbf{r})\,\mathbf{j}(\mathbf{r},t) \\ &\approx \frac{e}{m}\, n\mathbf{v}_\mathrm{o}(0)\langle 2|\mathbf{p}|1\rangle \exp(\mathrm{i}\Omega t)|2\rangle\langle 1| + \mathrm{H.c.} \\ &= \mathrm{i}en\Omega r_0 \exp(\mathrm{i}\Omega t)|2\rangle\langle 1| + \mathrm{H.c.}, \end{aligned}$$

where $n$ is the number of active atoms, $r_0 = \mathbf{v}_\mathrm{o}(0)\mathbf{r}_{21}$, and $\mathbf{r}_{21}$ is the matrix element of the electron coordinate for the transition $|2\rangle \to |1\rangle$.

The average excitation current of the output mode at the point in time $t$ is equal to

$$\begin{aligned} \langle j(t)\rangle = \mathrm{Sp}\left(j(t)\,\rho(t)\right) = \mathrm{i}en\Omega\big(r_\mathrm{o}\rho_{12}\exp(\mathrm{i}\Omega t) \\ - r_\mathrm{o}^*\rho_{12}^*\exp(-\mathrm{i}\Omega t)\big)\,, \end{aligned} \tag{3.12}$$

where $\rho_{12}(t)$ is the element of the atomic density matrix, the only one essential for the determination of the current.

**3.2.3 The field of the output mode.** We have been considering the case when the time of signal reception is smaller than the phase relaxation time; consequently, the relaxation can be disregarded at all. Then, it follows from Eqn (3.8) for the density matrix elements that

$$\begin{aligned} \rho_0(t) &= \rho_0(0) - \mathrm{i}\int_0^t \mathrm{d}t_1\left(\beta^*\rho_{01}^*(t_1) - \beta\rho_{01}(t_1)\right), \\ \rho_{01}(t) &= \rho_{01}(0) - \mathrm{i}\int_0^t \mathrm{d}t_1\left(\beta^*\rho_1(t_1) - \beta^*\rho_0(t_1) - \zeta\rho_{02}(t_1)\right), \\ \rho_{02}(t) &= \rho_{02}(0) - \mathrm{i}\int_0^t \mathrm{d}t_1\left(\beta^*\rho_{12}(t_1) - \zeta^*\rho_{01}(t_1)\right), \\ \rho_1(t) &= \rho_1(0) - \mathrm{i}\int_0^t \mathrm{d}t_1\left(\beta\rho_{01}(t_1) - \beta^*\rho_{01}^*(t_1)\right. \\ &\quad \left. + \zeta^*\rho_{12}^*(t_1) - \zeta\rho_{12}(t_1)\right), \\ \rho_{12}(t) &= \rho_{12}(0) - \mathrm{i}\int_0^t \mathrm{d}t_1\left(\beta\rho_{02}(t_1) + \zeta^*\rho_2(t_1) - \zeta^*\rho_1(t_1)\right), \\ \rho_2(t) &= \rho_2(0) - \mathrm{i}\int_0^t \mathrm{d}t_1\left(\zeta\rho_{12}(t_1) - \zeta^*\rho_{12}^*(t_1)\right). \end{aligned} \tag{3.13}$$

Let us assume that the signal being detected is a weak one, and the population of the lower level varies insignificantly over the entire time interval of interest and remains close to unity. Then, the element $\rho_{12}(t)$ of the density matrix appears in the third order of the perturbation theory:

$$\rho_{12}(t) = \mathrm{i}|\beta|^2 t\int_0^t \mathrm{d}t_1\, t_1\left(\alpha^* + \gamma^*(t_1)\right). \tag{3.14}$$

Therefore, in accordance with relationships (3.3), (3.12), and (3.14), the field of the output mode is described by the equation

$$\dot{u}(t) = -2\pi\mathrm{i}ecnr_\mathrm{o}^*|\beta|^2 t\int_0^t \mathrm{d}t_1\, t_1\left(\alpha + \gamma(t_1)\right).$$

In order to go over from $u(t)$ to $\gamma(t)$, let us multiply this equation, in accordance with formulas (3.10), by $-\mathrm{i}e\Omega r_\mathrm{o}/\hbar c$:

$$\dot{\gamma} = -\xi^2 t\int_0^t \mathrm{d}t_1\, t_1(\alpha + \gamma(t_1))\,, \tag{3.15}$$

where

$$\xi^2 = \frac{2\pi}{\hbar c}\,\varepsilon^2\Omega\omega^2 n|r_\mathrm{o}|^2|r_\mathrm{i}|^2|u_\mathrm{i}|^2\,, \tag{3.16}$$

and $\varepsilon$ is the fine-structure constant. Taking into account that

$$|u_\mathrm{i}|^2 = \frac{2\pi\hbar c^2 N}{\omega}\,,$$

where $N$ is the number of photons in the signal mode, the following expression is obtained for $\xi^2$:

$$\xi^2 = (2\pi)^2\varepsilon^2 v_\mathrm{o}^2 v_\mathrm{i}^2|r_{21}|^2|r_{10}|^2\omega\Omega c^2 nN\,. \tag{3.17}$$

The division of Eqn (3.14) by $t$ and differentiation of the resulting equality with respect to $t$ yield the equation

$$t\ddot{\gamma} - \dot{\gamma} + \xi^2 t^3\gamma + \xi^2 t^3\alpha = 0\,. \tag{3.18}$$

The general solution of equation (3.18) is written down as

$$\gamma(t) = -\alpha + A\sin\frac{\xi t^2}{2} + B\cos\frac{\xi t^2}{2}\,, \tag{3.19}$$

which can be verified by the direct substitution of expression (3.15) into this equation. Because at the instant of time when the signal appears, $\gamma(0) = 0$ and $\gamma(t)/t\big|_{t=0} = 0$ [as can be seen, for instance, from Eqn (3.9)], then $A = 0$ and $B = \alpha$. Therefore, the response of the system to the incoming signal is described by the relationship

$$\dot{\gamma}(t) = -\alpha\left(1 - \cos\frac{\xi t^2}{2}\right). \tag{3.20}$$

This means that after the arrival of the external signal, i.e., after producing the field $u_\mathrm{i}$, the field in the output mode builds up over time $\tau = \sqrt{2\pi/\xi}$ to a value roughly equal to the pump field that is much greater than the signal field. This characteristic response time $\tau$ of the detector must be smaller than or equal to the phase relaxation time $\tau_0$. The quantity $\xi^2$ can be represented in the form

$$\xi^2 = \left(\frac{e^2}{\hbar c}\right)^2 \frac{(2\pi c)^4|r_\mathrm{o}|^2|r_\mathrm{i}|^2}{V_\mathrm{i}\lambda_\mathrm{i}V_\mathrm{o}\lambda_\mathrm{o}}\,Nn\,, \tag{3.21}$$

where $n$ is the number of atoms interacting with the modes, $N$ is the number of photons in the signal mode, $V_\mathrm{i}$, $V_\mathrm{o}$ are the volumes of the signal and output modes, and $\lambda_\mathrm{i}$, $\lambda_\mathrm{o}$ are the wavelengths of the signal and the output radiation, respectively. Assuming that $\tau \approx \tau_0$, formula (3.21) determines the minimal number of photons that must be emitted in the signal mode to ensure that the field amplitude in the output mode could reach its maximum value during the detection time on the order of $\tau_0$. In other words, this parameter evaluates the sensitivity of the scheme under consideration with respect to the magnitude of the signal being received.

**3.2.4 Estimates.** In what follows, it is assumed that the phase relaxation time amounts to $\tau \approx 10^{-8}$ s. Evidently, such a time of transverse relaxation can be reached by cooling the active medium to the liquid-nitrogen temperature.

If $\xi^2 = (2\pi)^2/\tau_0^4$ and the number of photons in the signal mode equals

$$N = \frac{V_\mathrm{o}\lambda_\mathrm{o}V_\mathrm{i}\lambda_\mathrm{i}}{(2\pi)^2\varepsilon^2 c^4|r_{12}|^2|r_{01}|^2 n\tau_0^4}\,, \tag{3.22}$$

where $\varepsilon$ is the fine-structure constant, the field in the output mode builds up to its maximum value in a time $\tau_0$. For the purpose of estimation, the transverse dimensions of the mode are taken to be on the order of the wavelength $\lambda$, and its longitudinal size on the order of $10^2\lambda$. The dimensions of the two modes are roughly identical. As mentioned above, time $\tau_0$ is approximately $10^{-8}$ s. The concentration of active atoms amounts to $n_0 \approx 5 \times 10^{19}$ cm$^{-3}$, and their total number $n = n_0 V$. The matrix elements are estimated as $|r|^2 \approx 2 \times 10^{-19}$ cm$^2$ [35]. Then, in accordance with formula (3.21), if the number of photons in the signal mode is $N \approx 10^{-8}$, the field in the output mode reaches its maximum value in a time $\tau_0 \approx 10^{-8}$ s. As mentioned above, the maximum field in the output mode is approximately equal to the field in the pump mode. The pump mode can contain, say, ten photons. Consequently, the energy gain of the signal may be very high. Certainly, the realization of such sensitivities would require serious experimental efforts and theoretical analysis of the quantum nature of the signal being detected.

It was estimated that the number of spurious photons in the signal mode at frequency $\omega$ (resulting, for example, from the nonresonant Rayleigh scattering or from the nonresonant Raman scattering) is at least two orders of magnitude smaller than the above $N$ value.

One important note is in order. It was implicitly assumed in relationship (3.13) that all active ions are located at the same place of the resonant cavity. However, modes in optical resonators are known to be spatially distributed and, in particular, their phase varies from one point to another. In this case, the output and pump modes may be in phase at some points, and out of phase in another. In the event of uniform spatial distribution in the cavity, the evolving active ions follow the phase of the pump mode and can excite the output mode in one place but suppress the existing excitation in another. This accounts for the very weak overall interaction between the modes. For this reason, the distribution of active ions should not be uniform. They must be present only at those places of the cavity where the output and pump modes are in phase.

The aforesaid is illustrated by a simple example. Let us consider a dielectric cylindrical resonator (Fig. 11), with the output and pump modes assumed to be the so-called 'whispering gallery' modes, i.e., modes sliding around the circumference of the cylindrical surface of the cavity. The fields of such modes are described by the high-order Bessel functions.

For the sake of certainty, let the output mode be described by the distribution ($\varphi$ is the field point azimuth)

$$E_{mn}(r, \varphi) = J_m(\alpha_{mn} r) \sin m\varphi \,.$$

By virtue of the boundary condition, the following relation must be fulfilled at the cylindrical surface:

$$\alpha_{mn} r_c = \rho_{mn} \,,$$

where $\rho_{mn}$ is the $n$th root of the Bessel function derivative $J'_m(\rho_{mn}) = 0$. Evidently, the phase of this field depends on the azimuth. By analogy, let the pump mode be described by a similar distribution with other values of $m$ and $n$. The resonant frequencies of these modes may coincide at certain selected values of $m$ and $n$.

If the cavity diameter is taken, for certainty, to be 100 μm and its height 10 μm, it is easy to show that the output mode

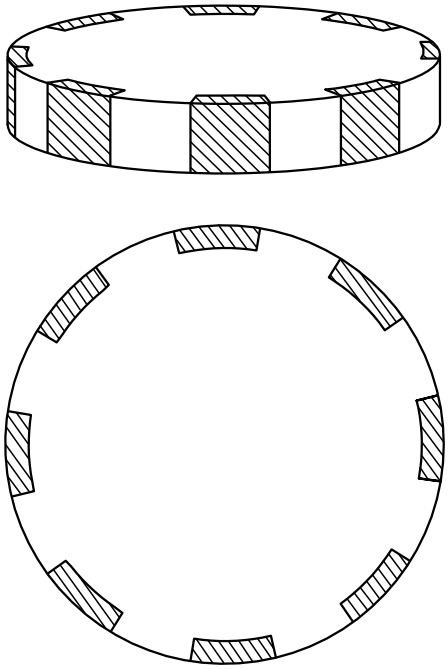

**Figure 11.** A resonant cavity for laser detection of optical signals; active atoms must be located in shaded areas where the pump and output modes are in-phase.

with indices $m = 314$ and $n = 1$ and the pump mode with indices $m' = 325$ and $n' = 0$ are degenerate, i.e., have identical resonant frequencies (corresponding to a wavelength on the order of 1 μm).

It is clear that the volume of the resonator adjoining its cylindrical surface will be divided into $\Delta m = m' - m$ $(11 = 325 - 314)$ sectors (see Fig. 11). In one half of each sector, the modes are in-phase, and in the other half out of phase. Active ions must be distributed only where the output and pump modes are in-phase (i.e., as shown in Fig. 11). Also, it should be borne in mind that the sign of the output mode varies with the radius; therefore, the depth of the ion distribution must not be larger than

$$\Delta = r_c - \frac{\rho_{m0}}{\alpha_{m1}} = r_c \left(1 - \frac{\rho_{m0}}{\rho_{m1}}\right) .$$

Given the above parameters of the resonant cavity, $\Delta$ is roughly 1.7 μm; at a greater depth, the output mode changes sign and turns out to be out of phase with the pump mode. The distribution of active ions shown in Fig. 11 ensures effective interaction between the modes. Certainly, it is only one possible variant of resonant cavities for the laser detection of weak optical signals.

**3.2.5 Summary.** We have demonstrated the possibility of laser detection of optical signals, at least in the absence of phase relaxation. It can be seen that the schemes proposed are very sensitive ones.

### 3.3 Large time of the detector response to the external signal. Consideration of phase relaxation

It will be shown in this section that phase relaxation time $T$, i.e., the time of the coherent interaction between the atom and the field, plays an important role in signal reception (such relaxation is also referred to as transverse). At long phase

relaxation times, the complete reception of a (pulsed) signal may take time $\tau$ which is smaller than $T$. This case has been considered in Section 3.2 (see also Refs [21, 22]). At small phase relaxation times, the reverse situation prevails — that is, the time $\tau$ of signal reception may be greater than $T$. We therefore consider below a case where the signal reception takes much more time than the phase relaxation time [22].

**3.3.1 Dynamics of active atoms in phase relaxation.** Phase relaxation is taken into account as usual, by matching the solutions together on separate coherence intervals where relaxation is insignificant. In this case, at the beginning of each interval, all nondiagonal elements of the density matrix of active atoms are set to zero, and all its diagonal elements are assumed to be continuous during the passage from one interval to another. In other words, phase relaxation is concentrated on an infinitely small time interval between separate coherence intervals. Also, it should be noted that only active atoms, not fields, undergo phase relaxation. Relaxation times for the fields are supposed to be much greater than all characteristic times of the problem in question.

Let us consider the solution to the system of equations (3.13) at nonzero initial diagonal elements

$$\rho_0(0) = \bar{\rho}_0 \neq 0\,, \qquad \rho_1(0) = \bar{\rho}_1 \neq 0\,, \qquad \rho_2(0) = \bar{\rho}_2 \neq 0\,,$$

assuming that they change insignificantly on the coherence time interval. Then, one finds

$$\rho_{12}(t) = -\mathrm{i}\bar{\zeta}^*(\bar{\rho}_2 - \bar{\rho}_1)t\,, \qquad \rho_{01}(t) = -\mathrm{i}\beta^*(\bar{\rho}_1 - \bar{\rho}_0)t \quad (3.23)$$

and

$$\begin{aligned} \Delta\rho_1 &= -|\beta|^2(\bar{\rho}_1 - \bar{\rho}_0)t^2 + |\bar{\zeta}|^2(\bar{\rho}_2 - \bar{\rho}_1)t^2\,, \\ \Delta\rho_2 &= -|\bar{\zeta}|^2(\bar{\rho}_2 - \bar{\rho}_1)t^2\,, \qquad \Delta\rho_0 = -|\beta|^2(\bar{\rho}_1 - \bar{\rho}_0)t^2\,, \end{aligned} \quad (3.24)$$

where the over-bar indicates quantities practically constant on the coherence interval and slowly varying on time intervals much larger than the characteristic coherence time $T$. For the diagonal elements of the density matrix, it is possible to introduce so-called slow or smoothed derivatives

$$\begin{aligned} &\frac{\mathrm{d}\rho_0}{\mathrm{d}t} = |\beta|^2 T(\rho_1 - \rho_0)\,, \qquad \frac{\mathrm{d}\rho_2}{\mathrm{d}t} = -\bigl|\zeta(t)\bigr|^2 T(\rho_2 - \rho_1)\,, \\ &\frac{\mathrm{d}\rho_1}{\mathrm{d}t} = -|\beta|^2 T(\rho_1 - \rho_0) + \bigl|\zeta(t)\bigr|^2 T(\rho_2 - \rho_1)\,. \end{aligned} \quad (3.25)$$

**3.3.2 Excitation current of the cavity.** The atomic current density is proportional to the electron momentum:

$$\mathbf{J}(\mathbf{r}, \mathbf{q}) = \frac{e}{m}\,\mathbf{p}\,\delta(\mathbf{r} - \mathbf{q})\,.$$

Accordingly, for the current of the $|1\rangle \leftrightarrow |2\rangle$ transition in the interaction representation, one has

$$\mathbf{j}(\mathbf{r}, t) = \frac{e}{m}\bigl(\langle 2|\mathbf{p}\,\delta(\mathbf{r} - \mathbf{q})|1\rangle\bigr)\exp(\mathrm{i}\Omega t)|2\rangle\langle 1| + \text{H.c.}$$

The average current of the $|1\rangle \leftrightarrow |2\rangle$ transition is equal to

$$\bigl\langle \mathbf{j}(\mathbf{r}, t)\bigr\rangle = \frac{e}{m}\bigl(\langle 2|\mathbf{p}\,\delta(\mathbf{r} - \mathbf{q})|1\rangle\bigr)\rho_{12}(t)\exp(\mathrm{i}\Omega t) + \text{c.c.}, \quad (3.26)$$

where c.c. is the complex conjugate term. This means that $\rho_{12}(t)$ is the sole important element of the density matrix to determine the current exciting the output mode.

Using Eqn (3.26) for the atomic transition current and the solution of Eqn (3.23), it is possible to calculate the amplitude of the negative-frequency part of the current:

$$\mathbf{j}' = \frac{\mathrm{i}e}{m}\langle 1|\mathbf{p}\,\delta(\mathbf{r} - \mathbf{q})|2\rangle\bar{\zeta}(\bar{\rho}_2 - \bar{\rho}_1)t\,.$$

Taking into consideration that

$$\mathbf{p}_{nl} = \mathrm{i}m\Omega_{nl}\mathbf{r}_{nl} \qquad (n > l)\,,$$

and integrating over $\mathbf{r}$ in accordance with expressions (3.2) lead to the result

$$j'(t) = en\Omega r_{\mathrm{o}}^*\bar{\zeta}(\bar{\rho}_2 - \bar{\rho}_1)t\,, \quad (3.27)$$

where it was taken into account that the cavity contains $n$ identical active atoms.

**3.3.3 The output mode field.** According to formulas (3.3) and (3.27), the increment of the negative-frequency part of the field amplitude on the coherence interval is equal to

$$\Delta u = \mathrm{i}\pi nec r_{\mathrm{o}}^*\,\bar{\zeta}(\bar{\rho}_1 - \bar{\rho}_2)T^2\,.$$

We multiply this relationship by $-\mathrm{i}e\Omega r_{\mathrm{o}}/\hbar c$ to go over to $\gamma$ and introduce for $\gamma$ the smoothed derivative

$$\dot{\gamma}(t) = S(\bar{\rho}_2 - \bar{\rho}_1)\bigl(\alpha + \gamma(t)\bigr)\,,$$

where

$$S = \pi\varepsilon|r_{\mathrm{o}}|^2 c\Omega Tn \qquad \left(\varepsilon = \frac{e^2}{\hbar c}\right). \quad (3.28)$$

Since $\alpha = \text{const}$, we arrive at the equation

$$\dot{\zeta}(t) = S(\bar{\rho}_2 - \bar{\rho}_1)\zeta\,. \quad (3.29)$$

This yields the following expression for $\zeta$:

$$\zeta(t) = \zeta_0\exp\left[-S\int_{t'}^{t''}\mathrm{d}t_1\,\bigl(\bar{\rho}_1(t_1) - \bar{\rho}_2(t_1)\bigr)\right]. \quad (3.30)$$

Notice that the integral in formula (3.30) can be extended over the time interval between the arrival of the signal to the system and a given point in time due to additivity of the exponents coming from individual coherence intervals:

$$\zeta(t) = \alpha\exp\left[-S\int_0^t\mathrm{d}t_1\,\bigl(\bar{\rho}_1(t_1) - \bar{\rho}_2(t_1)\bigr)\right]. \quad (3.31)$$

Hence, the solution sought is given by

$$\gamma(t) = -\alpha\left\{1 - \exp\left[S\int_0^t\mathrm{d}t_1\,\bigl(\rho_2(t_1) - \rho_1(t_1)\bigr)\right]\right\}. \quad (3.32)$$

**3.3.4 Population dynamics at active levels and the output field.** System of equations (3.25) can now be represented as

$$\begin{aligned} &\frac{\mathrm{d}\rho_0}{\mathrm{d}t} = B(\rho_1 - \rho_0)\,, \qquad \frac{\mathrm{d}\rho_2}{\mathrm{d}t} = -AZ(\rho_2 - \rho_1)\,, \\ &\frac{\mathrm{d}\rho_1}{\mathrm{d}t} = -B(\rho_1 - \rho_0) + AZ(\rho_2 - \rho_1)\,, \end{aligned} \quad (3.33)$$

where

$$B = |\beta|^2 T, \qquad A = |\alpha|^2 T, \qquad Z = |\zeta|^2 T. \tag{3.34}$$

The quantities $A$ and $B$, having dimension [$s^{-1}$], equal

$$A = 2\pi\varepsilon |r|^2 N c \Omega T, \qquad B = 2\pi\varepsilon |r_i|^2 N_i c \omega T, \tag{3.35}$$

where $N$ and $N_i$ are the numbers of photons in the pump and signal modes, respectively. The quantity $Z(t)$ equalling

$$Z(t) = \exp\left[-2S\int_0^t \mathrm{d}t_1 \left(\rho_1(t_1) - \rho_2(t_1)\right)\right]$$

is, in accordance with formula (3.32), a measure of excitation of the output mode; at $Z = 0$, the output mode turns out to be excited up to the level of a pump mode.

It follows from Eqns (3.33) that time-dependent changes in $Z(t)$ are determined by parameters $A$, $B$, and $S$. Therefore, their approximate values for practically realized media need to be known for estimating $Z(t)$. It should be noted that the parameters $A$ and $B$ are proportional to the number of photons in the pump and signal modes, respectively, and can vary under experimental conditions. The number of photons in the pump mode is taken to be 100; this number must not be too high to avoid strong nonlinear nonresonance phenomena in the medium. The number of photons in the signal mode is assumed to be unity in order to demonstrate the high sensitivity of the device being considered.

**3.3.5 Estimates.** Parameter $S$ is proportional to the number of active atoms in the medium filling the cavity. In experiment, it has a given value. For the purpose of estimation, the active medium is chosen to be neodymium-doped garnet [23] in which the active ion density measures $\approx 2 \times 10^{19}$ $cm^{-3}$ and $|r_{21}|^2 \approx 2 \times 10^{-19}$ $cm^2$. The volumes of all three modes are roughly identical, amounting to $\approx 10^3 \lambda^3 \approx 10^{-9}$ $cm^3$. In this case, one has

$$A \approx 4 \times 10^4 \ s^{-1}, \qquad B \approx 4 \times 10^2 \ s^{-1}, \qquad S \approx 2 \times 10^{12} \ s^{-1}.$$

Putting

$$\rho' = \rho_1 - \rho_0, \qquad \rho'' = \rho_2 - \rho_1.$$

in the system of equations (3.33), we then reduce this system to two equations

$$\frac{\mathrm{d}\rho'}{\mathrm{d}t} = -2B\rho' + AZ\rho'', \qquad \frac{\mathrm{d}\rho''}{\mathrm{d}t} = B\rho' - 2AZ\rho''$$

with

$$Z(t) = \exp\left[2S\int_0^t \mathrm{d}t_1 \, \rho''(t_1)\right].$$

For our purposes, it is sufficient to consider only the initial time interval in which the ground-state amplitude remains virtually unaltered, i.e., $\rho'(t) \approx -1 = \text{const}$. Then, in the second equation, it is sufficient to take into account only the first term on the right-hand side. Indeed, the second term may become roughly equal to the first one over the time $1/2A$ ($\approx 10^{-5}$ s) at $Z = 1$. Meanwhile, $Z(t)$ will practically vanish much sooner. Actually, one obtains at the initial stage that

$$\rho'' \approx -Bt, \qquad Z(t) \approx \exp\left(-SBt^2\right).$$

Thus, $Z(t)$ diminishes according to the Gaussian law with the characteristic time

$$\tau = \frac{1}{\sqrt{SB}} \approx 3 \times 10^{-8} \ \mathrm{s};$$

during this time, the quantity $\rho'$ changes only by $10^{-7}$.

It may be concluded that under the influence of a weak signal the output mode is excited up to the level of the pump mode during the time $\tau$. This means that the scheme considered possesses large gain. In the presence of relaxation, the detection process is virtually the same as in its absence (see Section 3.2). Naturally, the detector's response time to a signal in the presence of relaxation is slightly greater than in its absence.

## 4. Conclusions

The discussion of the nature of photocounts in the first part of this review has demonstrated that they are caused by the instability of a low electron flux induced in a photodetector by the received radiation. This explains the main properties of photocounts.

The possible scheme of detecting optical signals with laser tools as described in Section 3 appears to withstand the effect of phase relaxation processes in the medium. It is shown that such schemes can be highly sensitive.

The most remarkable feature of the discussed laser detection schemes is their ability to fix portions of energy equivalent to small fractions of a quantum of the radiation being received. Practical realization of this ability may radically change the situation in the quantum theory of measurements.

Another important property of laser detectors is their ability to record weak optical signals without photocounts because electron excitation is distributed in them over many active atoms possessing electron subsystems well stabilized by a strong Coulomb nuclear field. This means that shot noises in laser detectors are strongly suppressed. The physical nature of these noises is quite different from that in conventional radiation detectors.

The author is grateful to A M Prokhorov, F V Bunkin, E M Dianov, Yu V Gulyaev, I A Shcherbakov, M A Ananyan, A N Oraevsky, L A Rivlin, Yu K Voron'ko, G Kh Kitaeva, Yu D Golyaev, A V Masalov, V V Savransky, and I V Pryanikov for discussions on the results of the study. Special thanks are due to A V Gerasimov and V O Turin, the author's postgraduate students, who greatly contributed to the development of the research presented; it was easy and gratifying to work with them. The study was supported by the Russian Foundation for Basic Research (grants Nos 98-02-16671 and 01-02-17479).

## 5. Appendices

### Appendix 1. Spherically symmetric expansion of an electron bunch

Let a spherically symmetric distribution of the charge density $\sigma(r)$ be given initially, while the bunch is at rest — that is, the velocities at all points of the bunch are zero. Then, the electric field $E(R)$ on a sphere with radius $R$ is given by

$$E(R) = \frac{Q(R)}{R^2}, \tag{A1.1}$$

where $Q(R)$ is the total charge enclosed by this sphere:

$$Q(R) = 4\pi \int_0^R \mathrm{d}r\, r^2 \sigma(r)\,. \tag{A1.2}$$

It should be pointed out that prior to the onset of overtaking, the quantity $Q(R)$ is a constant, i.e., $Q(R) = Q(R_0)$ if $R_0$ is the initial value of $R$. Therefore, the law of motion for charges lying on the sphere of radius $R$ has the form

$$m\ddot{R} = \frac{eQ(R_0)}{R^2}\,. \tag{A1.3}$$

Also suppose that, in addition, the charge distribution is Gaussian at the initial moment:

$$\sigma(\mathbf{r}) = \frac{Q_0}{\pi^{3/2} r_0^3} \exp\left(-\frac{r^2}{r_0^2}\right), \tag{A1.4}$$

where $Q_0$ is the total distributed charge. Then, integration of this equation yields the dependence

$$\left\{\left[\rho(\rho-\rho_0)\right]^{1/2} + \rho_0 \ln \frac{(\rho-\rho_0)^{1/2} + \rho^{1/2}}{\rho_0^{1/2}}\right\}\left(\frac{\rho_0}{I(\rho_0)}\right)^{1/2} = \tau\,, \tag{A1.5}$$

where

$$\rho = \frac{R}{r_0}\,, \qquad \rho_0 = \frac{R_0}{r_0}\,, \qquad \tau = \frac{t}{t_0}\,, \tag{A1.6}$$

$$t_0 = \left(\frac{m}{e}\frac{r_0^3}{Q_0}\right)^{1/2}, \quad I(\rho_0) = \frac{4}{\pi^{1/2}} \int_0^{\rho_0} \mathrm{d}\rho\, \rho^2 \exp\left(-\rho^2\right). \tag{A1.7}$$

Let us now investigate how the charge density $\sigma(R)$ varies with time. It should be noted that up to the onset of overtaking, the total charge enclosed in a thin spherical layer of thickness $\mathrm{d}R$ is conserved in the course of time. Hence, the equality

$$\sigma(R) R^2\, \mathrm{d}R = \sigma(R_0) R_0^2\, \mathrm{d}R_0$$

is satisfied or

$$\sigma(R) = \sigma(R_0)\, \frac{R_0^2}{R^2}\, \frac{\mathrm{d}R_0}{\mathrm{d}R}\,. \tag{A1.8}$$

It follows from this relationship that the charge density may be regarded as infinite only if the derivative $\mathrm{d}R_0/\mathrm{d}R$ becomes infinite, too, or if $\mathrm{d}R/\mathrm{d}R_0$ vanishes (which is the same).

The derivative $\mathrm{d}R_0/\mathrm{d}R$ can be found by differentiating the relation (A1.5) with respect to $R_0$:

$$\dot{R} = \rho - \frac{1}{2}\left\{(\rho-1) + \left(\frac{\rho-1}{\rho}\right)^{1/2} \ln\left[(\rho-1)^{1/2} + \rho^{1/2}\right]\right\} \frac{3 - R_0 Q}{Q}\,. \tag{A1.9}$$

The dependence of $R$ on $R_0$ was calculated with a computer and the $R$-dependent charge density was found from relations (A1.8) and (A1.9). This dependence for different time instants is displayed in Fig. 6.

At a point where the derivative $\mathrm{d}R/\mathrm{d}R_0$ vanishes for the first time, the dependence $R(R_0)$ has an inflection and can be represented in the form

$$R(R_0) = B + \varepsilon(R_0 - A)^3 + \ldots, \tag{A1.10}$$

where $A$ and $B$ are certain constants. Then, $R_0$ depends on $R$ as follows:

$$R_0(R) = A + \left(\frac{R-B}{\varepsilon}\right)^{1/3}. \tag{A1.11}$$

The derivative $\mathrm{d}R/\mathrm{d}R_0$ near this point takes the form

$$\frac{\mathrm{d}R}{\mathrm{d}R_0} = 3\varepsilon(R_0 - A)^2 = 3\varepsilon^{1/2}(R-B)^{2/3}\,. \tag{A1.12}$$

Thus, the $R$-dependence of the charge density in the vicinity of the point where it becomes infinite can be represented as

$$\sigma(R) = \frac{1}{3}\, \sigma(A) \varepsilon^{-1/2} \left(\frac{A}{B}\right)^2 (R-B)^{-2/3}\,. \tag{A1.13}$$

It can be seen that initially $R$ and $R_0$ are identical. Thereafter, the bunch begins to expand and the charges on the charge distribution slope have the highest velocities and, consequently, are displaced the largest distances. As a result, the preceding layers overtake the following ones. For example, displacements at $R_0 \approx 1.5$ are considerably greater than that at $R_0 \approx 2.0$ [6]. For $t = 2.77$, the values of $R$ corresponding to $1.5 < R < 2.0$ become equalized, which implies the beginning of overtaking and an increase in the charge density until it becomes infinite. Figure 4 demonstrates the formation of a maximum in the charge density distribution and its sharpening with time near $R \approx 3.65$. The peak density at $t = 2.77$ is almost four orders of magnitude greater than at the center of the distribution. It tends to infinity if electron wave properties are disregarded.

## Appendix 2. Movement of an electron wave packet in an electromagnetic field

It has been shown in this review that isolated electron wave packets in vacuum photodetectors, such as photomultipliers, have a relatively large size and, thus, can be observed with the help of modern technical means. It has also emerged from the discussion of the nature and mechanisms of formation of such wave packets that their possible cause is the Coulomb instability of a quasi-uniform low-density electron flux.

In this context, it is of interest to consider movements of electron wave packets in electromagnetic fields of a sufficiently general form on the sole condition (always fulfilled in the aforementioned devices) that the characteristic size of the spatial variations of these fields be substantially larger than the characteristic size of the packets. In this case, the fields inside the packet and in its immediate neighborhood can be expanded in a series and in the calculations made we take into account only the terms of the zero, first, and second orders with respect to displacements of the points of the packet from its center. It turns out that in this approximation the center of the packet moves along a classical trajectory, and the matrix of its parameters obeys a Riccati-type matrix equation. In what follows, the derivation of this equation is described, its properties are discussed, and a simple example of the packet motion in a uniform magnetic field is considered. Special cases of this equation are dealt with in Refs [6, 9, 10].

The Hamiltonian that describes the wave packet motion has the following form

$$H = \frac{1}{2m}\left(\mathbf{p} - \frac{e}{c}\,\mathbf{A}(\mathbf{r})\right)^2 + eU(\mathbf{r})\,,$$

where $\mathbf{p}$, $\mathbf{r}$ are the momentum and the coordinate of the electron, and $\mathbf{A}(\mathbf{r},t)$, $U(\mathbf{r},t)$ are the vector and the scalar field potentials, respectively, that are actually the given functions of the coordinates and time. This Hamiltonian is known to yield ordinary classical equations of motion for a point electron:

$$\begin{aligned}\dot{\mathbf{r}} &= \frac{1}{m}\left(\mathbf{p} - \frac{e}{c}\,\mathbf{A}(\mathbf{r})\right),\\ \dot{\mathbf{p}} &= -\frac{1}{2m}\,\mathrm{grad}\left(\mathbf{p} - \frac{e}{c}\,\mathbf{A}(\mathbf{r})\right)^2 - e\,\mathrm{grad}\,U(\mathbf{r})\,,\end{aligned} \tag{A2.1}$$

which, in the Newtonian representation, take the form

$$m\ddot{\mathbf{r}} = e\mathbf{E}(\mathbf{r},t) + \frac{e}{c}\left[\dot{\mathbf{r}} \times \mathbf{H}(\mathbf{r},t)\right],$$

where $\mathbf{E}(\mathbf{r},t)$ and $\mathbf{H}(\mathbf{r},t)$ are the electric and the magnetic fields, respectively, so that

$$\mathbf{E}(\mathbf{r},t) = -\frac{1}{c}\,\frac{\partial \mathbf{A}(\mathbf{r},t)}{\partial t} - \mathrm{grad}\,U(\mathbf{r},t)\,, \qquad \mathbf{H}(\mathbf{r},t) = \mathrm{rot}\,\mathbf{A}(\mathbf{r},t)\,.$$

Let us consider the motion of an electron wave packet in an electromagnetic field, when the characteristic size of field inhomogeneity markedly exceeds the packet dimensions. For this purpose, the solution of the Schrödinger equation should be sought in the form of a Guassian wave packet:

$$\begin{aligned}\Psi(\mathbf{r},t) &= C\exp\left\{-(\boldsymbol{\rho}, F\boldsymbol{\rho}) + \frac{\mathrm{i}}{\hbar}\left[\mathbf{p}_0(t)\boldsymbol{\rho} + E(t)\right]\right\},\\ C &= \left[\left(\frac{2}{\pi}\right)^3 \det \mathrm{Re}\,F(0)\right]^{1/4},\end{aligned} \tag{A2.2}$$

where $F(t)$ is the complex symmetric $3\times 3$ matrix, $\boldsymbol{\rho} = \mathbf{r} - \mathbf{r}_0(t)$, and the parameters $\mathbf{r}_0(t)$ and $\mathbf{p}_0(t)$ describe the motion of the wave packet center. In case of the Coulomb gauge, namely

$$\mathrm{div}\,\mathbf{A}(\mathbf{r},t) = 0\,, \qquad \Delta U(\mathbf{r},t) = 0\,,$$

the Schrödinger equation has the form

$$\mathrm{i}\hbar\,\frac{\partial \Psi}{\partial t} = \left[\frac{1}{2m}\,\mathbf{p}^2 + eU(\mathbf{r}) - \frac{e}{mc}\,\mathbf{A}(\mathbf{r})\mathbf{p} + \frac{e^2}{2mc^2}\,\mathbf{A}^2(\mathbf{r})\right]\Psi\,. \tag{A2.3}$$

The substitution of the wave packet (A2.2) into this equation, followed by its division by the same relationship (A2.2), yields the expression

$$\mathrm{i}\hbar\left[-(\boldsymbol{\rho}, \dot{F}\boldsymbol{\rho}) + 2(\dot{\mathbf{r}}_0, F\boldsymbol{\rho}) + (\dot{\mathbf{p}}_0\boldsymbol{\rho} - \mathbf{p}\dot{\mathbf{r}}_0 + \dot{E})\right]$$

on the left-hand side of the Schrödinger equation; this expression contains $\boldsymbol{\rho}$-independent and linear terms as well as terms quadratic in $\boldsymbol{\rho}$. Taking into consideration the expansions for the scalar and vector potentials

$$\begin{aligned}U(\mathbf{r}) &\approx U(\mathbf{r}_0) + (\boldsymbol{\rho}\boldsymbol{\nabla})\,U(\mathbf{r}_0) + \frac{1}{2!}(\boldsymbol{\rho}\boldsymbol{\nabla})^2 U(\mathbf{r}_0) + \ldots,\\ \mathbf{A}(\mathbf{r}) &\approx \mathbf{A}(\mathbf{r}_0) + (\boldsymbol{\rho}\boldsymbol{\nabla})\,\mathbf{A}(\mathbf{r}_0) + \frac{1}{2!}(\boldsymbol{\rho}\boldsymbol{\nabla})^2 \mathbf{A}(\mathbf{r}_0) + \ldots,\end{aligned}$$

the right-hand side of the Schrödinger equation can also be represented as the sum of the $\boldsymbol{\rho}$-independent, linear and quadratic in $\boldsymbol{\rho}$ terms. The collection of terms that do not contain $\boldsymbol{\rho}$ gives an equation that defines the function $E(t)$:

$$\dot{E} = \frac{1}{2m}\,\mathbf{p}_0^2 - eU(\mathbf{r}_0) - \frac{e^2}{2mc^2}\,\mathbf{A}^2(\mathbf{r}_0) - \frac{\hbar^2}{m}\,\mathrm{Sp}\,F\,.$$

Similarly, collecting terms of the first order with respect to $\boldsymbol{\rho}$ gives the Hamiltonian equations (A2.1) for the parameters $\mathbf{r}_0(t)$, $\mathbf{p}_0(t)$. It means that the center of the wave packet moves along the classical trajectory. The terms of a second-order smallness in $\boldsymbol{\rho}$ yield

$$\begin{aligned}-\mathrm{i}\hbar(\boldsymbol{\rho}, \dot{F}\boldsymbol{\rho}) &= \frac{2\hbar^2}{m}(\boldsymbol{\rho}, F^2\boldsymbol{\rho}) + \frac{1}{2}\,e(\boldsymbol{\rho}\boldsymbol{\nabla})^2 U(\mathbf{r}_0)\\ &- \frac{2\mathrm{i}e\hbar}{mc}\left[(\boldsymbol{\rho}\boldsymbol{\nabla})\,\mathbf{A}(\mathbf{r}_0)\right]F\boldsymbol{\rho}\\ &- \frac{e}{2mc}\left(\mathbf{p}_0 - \frac{e}{c}\,\mathbf{A}(\mathbf{r}_0)\right)\left[(\boldsymbol{\rho}\boldsymbol{\nabla})^2\,\mathbf{A}(\mathbf{r}_0)\right] + \frac{e^2}{2mc^2}\left[(\boldsymbol{\rho}\boldsymbol{\nabla})\,\mathbf{A}(\mathbf{r}_0)\right]^2.\end{aligned}$$

By reducing all the terms in this expression to the standard form

$$(\boldsymbol{\rho}, M\boldsymbol{\rho})\,,$$

where $M$ is a certain $3\times 3$ matrix, we obtain the following nonlinear equation of the Riccati type for the matrix $F$:

$$\begin{aligned}\mathrm{i}\hbar\,\frac{\partial F}{\partial t} &= \frac{2\hbar^2}{m}\,F^2 + \frac{\mathrm{i}e\hbar}{mc}\left[d\big(\mathbf{A}(\mathbf{r}_0)\big)F + Fd^{\mathrm{T}}\big(\mathbf{A}(\mathbf{r}_0)\big)\right]\\ &- \frac{e^2}{2mc^2}\left[d\big(\mathbf{A}(\mathbf{r}_0)\big)\,d^{\mathrm{T}}\big(\mathbf{A}(\mathbf{r}_0)\big)\right]\\ &- \frac{1}{2}\,e\,D_2U(\mathbf{r}_0) + \frac{e}{2c}\left(\dot{\mathbf{r}}_0\,D_2\mathbf{A}(\mathbf{r}_0)\right),\end{aligned} \tag{A2.4}$$

where $d\big(\mathbf{A}(\mathbf{r}_0)\big)$, $D_2\mathbf{A}(\mathbf{r}_0)$, $D_2U(\mathbf{r}_0)$ are the matrices defined by spatial derivatives of the potentials with respect to components of $\mathbf{r}_0$:

$$d\big(\mathbf{A}(\mathbf{r}_0)\big) = \begin{pmatrix} \dfrac{\partial A_x}{\partial x} & \dfrac{\partial A_y}{\partial x} & \dfrac{\partial A_z}{\partial x}\\ \dfrac{\partial A_x}{\partial y} & \dfrac{\partial A_y}{\partial y} & \dfrac{\partial A_z}{\partial y}\\ \dfrac{\partial A_x}{\partial z} & \dfrac{\partial A_y}{\partial z} & \dfrac{\partial A_z}{\partial z}\end{pmatrix},$$

$$D_2\mathbf{A}(\mathbf{r}_0) = \begin{pmatrix} \dfrac{\partial^2 \mathbf{A}}{\partial x^2} & \dfrac{\partial^2 \mathbf{A}}{\partial x\,\partial y} & \dfrac{\partial^2 \mathbf{A}}{\partial x\,\partial z}\\ \dfrac{\partial^2 \mathbf{A}}{\partial y\,\partial x} & \dfrac{\partial^2 \mathbf{A}}{\partial y^2} & \dfrac{\partial^2 \mathbf{A}}{\partial y\,\partial z}\\ \dfrac{\partial^2 \mathbf{A}}{\partial z\,\partial x} & \dfrac{\partial^2 \mathbf{A}}{\partial z\,\partial y} & \dfrac{\partial^2 \mathbf{A}}{\partial z^2}\end{pmatrix},$$

$$D_2U(\mathbf{r}_0) = \begin{pmatrix} \dfrac{\partial^2 U}{\partial x^2} & \dfrac{\partial^2 U}{\partial x\,\partial y} & \dfrac{\partial^2 U}{\partial x\,\partial z}\\ \dfrac{\partial^2 U}{\partial y\,\partial x} & \dfrac{\partial^2 U}{\partial y^2} & \dfrac{\partial^2 U}{\partial y\,\partial z}\\ \dfrac{\partial^2 U}{\partial z\,\partial x} & \dfrac{\partial^2 U}{\partial z\,\partial y} & \dfrac{\partial^2 U}{\partial z^2}\end{pmatrix}.$$

These matrices are the time functions because $\mathbf{r}_0 = \mathbf{r}_0(t)$, in conformity with equation (A2.1).

The introduction of a new matrix $\Phi$ instead of $F$, namely

$$F = \frac{m}{2\hbar}\,\Phi\,, \qquad \Phi = \frac{2\hbar}{m}\,F\,,$$

leads to

$$\mathrm{i}\dot{\Phi} = \Phi^2 + \frac{\mathrm{i}e}{mc}\big(d(\mathbf{A})\Phi + \Phi d^{\mathrm{T}}(\mathbf{A})\big) - \frac{e}{m}\,D_2U - \frac{e^2}{m^2c^2}\big(d(\mathbf{A})\,d^{\mathrm{T}}(A)\big) + \frac{e}{mc}(\dot{\mathbf{r}}_0 D_2\mathbf{A})\,. \tag{A2.5}$$

Notice that we may do away with the Coulomb gauge of the potentials. For this, the vector potential $\mathbf{A}(\mathbf{r}_0)$ in the last term of Eqn (A2.5) must be substituted by its eddy, i.e., transverse, part $\mathbf{A}^{\perp}(\mathbf{r}_0)\big(\mathrm{div}\,A(\mathbf{r}_0) = 0\big)$.

Although the matrix equation (A2.5) of the Riccati type is nonlinear, it can be reduced (for an arbitrary $n \times n$ dimension) to a set of linear equations. For this, a system of such equations

$$\frac{\mathrm{d}X}{\mathrm{d}t} = A_1X + A_2Y\,, \qquad \frac{\mathrm{d}Y}{\mathrm{d}t} = A_3X + A_4Y \tag{A2.6}$$

should be considered, where $X$, $Y$ are the $n$-component vectors, and $A_i$ are the $n \times n$ matrices (arbitrary time functions). System (A2.6) has $n$ linearly independent solutions that can be regarded as columns of the matrices $\hat{X}$, $\hat{Y}$. It is demanded that initially matrix $\hat{Y}$ be unit and matrix $\hat{X}$ be coincident with $\Phi(0) = \Phi_0$. The solution of system (A2.6) under the boundary conditions said (which is not always simple) leads to $n \times n$-matrices $X(t)$ and $Y(t)$. These matrices, in the same way as vectors $X$, $Y$, satisfy equations (A2.6). Matrix $\Phi(t)$ is defined by the equality

$$\Phi(t) = X(t)\,Y^{-1}(t)\,; \tag{A2.7}$$

evidently, this matrix has an initial value equal to $\Phi_0$. Differentiating this expression with respect to time and making use of Eqn (A2.6) convinces us that the matrix $\Phi(t)$ obeys the equation

$$\dot{\Phi} = -\Phi A_3\Phi + A_1\Phi - \Phi A_4 + A_2\,, \tag{A2.8}$$

i.e., a nonlinear matrix equation of the Riccati type. In this way, having found the solutions of the linear system (A2.6), it is possible to solve the nonlinear matrix equation (A2.8) with the help of relationship (A2.7).

It is easy to see that Eqn (A2.5) for $\Phi$ represents equations of the (A2.8) type; indeed, it converts into (A2.8) at $n = 3$ and

$$A_1 = \frac{e}{mc}\,d(\mathbf{A})\,,$$

$$A_2 = \mathrm{i}\left[\frac{e}{m}\,D_2U + \frac{e^2}{m^2c^2}\big(d(\mathbf{A})\,d^{\mathrm{T}}(\mathbf{A})\big) - \frac{e}{mc}(\dot{\mathbf{r}}_0\,D_2\mathbf{A})\right],$$

$$A_3 = -\mathrm{i}I\,, \qquad A_4 = -\frac{e}{mc}\,d^{\mathrm{T}}(\mathbf{A})\,.$$

It can be proven that the solution of Eqn (A2.7) for the matrix $\Phi(t)$ remains invariably symmetric, provided the initial matrix $\Phi_0$ is symmetric, too.

Let us consider, by way of illustration, the motion of a wave packet in a longitudinal, uniform, and constant, magnetic field described by the vector potential

$$\mathbf{A}(\mathbf{r}) = \frac{1}{2}\,H(-y, x, 0) \qquad \big(\mathrm{div}\,\mathbf{A}(\mathbf{r}) = 0\big)\,.$$

In this case, we have

$$d\big(\mathbf{A}(\mathbf{r}_0)\big) = \frac{1}{2}\,H\begin{pmatrix} 0 & 1 & 0 \\ -1 & 0 & 0 \\ 0 & 0 & 0 \end{pmatrix}$$

and $D_2\mathbf{A}(\mathbf{r}_0) = D_2U(\mathbf{r}_0) = 0$. It can be seen that the longitudinal distribution of the packet behaves as in a free space. For the transverse components, there is equation

$$\mathrm{i}\dot{\bar{\Phi}} = \bar{\Phi}^2 + \mathrm{i}\Omega(\sigma\bar{\Phi} + \bar{\Phi}\sigma^{\mathrm{T}}) - \Omega^2 I\,, \tag{A2.9}$$

where $\bar{\Phi}$ is the $2 \times 2$ matrix, and

$$\sigma = \begin{pmatrix} 0 & 1 \\ -1 & 0 \end{pmatrix},$$

and $\Omega = eH/2mc$ is the Larmor precession frequency.

In a special case, when the wave packet is axially symmetric about its rectilinear trajectory, matrix $\bar{\Phi}$ can be proportional to the identity matrix:

$$\bar{\Phi} = \Omega W(\tau) I\,,$$

while

$$\tau = \Omega t\,, \qquad I = \begin{pmatrix} 1 & 0 \\ 0 & 1 \end{pmatrix},$$

and $W(\tau)$ obeys the equation

$$W' = \mathrm{i}(1 - W^2)\,,$$

where the prime denotes differentiation with respect to $\tau$. This equation has the solution

$$W(t) = \frac{(1 + W_0)\exp(\mathrm{i}\Omega t) - (1 - W_0)\exp(-\mathrm{i}\Omega t)}{(1 + W_0)\exp(\mathrm{i}\Omega t) + (1 - W_0)\exp(-\mathrm{i}\Omega t)}\,,$$

where $W_0$ is the initial value of $W(t)$. The real part of $W(t)$ is given by

$$\mathrm{Re}\,W(t) = \frac{W_1}{(\cos\Omega t - W_2\sin\Omega t)^2 + W_1^2\sin^2\Omega t}\,,$$

where $W_1$, $W_2$ are the real and the imaginary parts of $W_0$, respectively. Thus, the transverse dimensions of the wave packet oscillate with the double Larmor frequency. The maximum and minimum values of $\mathrm{Re}\,W(t)$ equal $W_1$ and $(1 + W_2^2)/W_1$, respectively. When $W_0$ is unity, then the solution is stationary — that is, a wave packet of the transverse size

$$d = 2\sqrt{\frac{\hbar c}{eH}} = \sqrt{\frac{2\hbar}{m\Omega}}$$

retains its dimensions when travelling in a longitudinal magnetic field. There is another, less symmetric solution of Eqn (A2.9) that describes wave packets flattened in the transverse direction:

$$\bar{\Phi} = \Omega\begin{pmatrix} 1 + Z & \mathrm{i}Z \\ \mathrm{i}Z & 1 - Z \end{pmatrix},$$

where $Z$ is the arbitrary complex number ($|Z| < 1$). This solution can be simplified by rotating the axes through the

angle $\varphi/2$, where $\varphi = \arg Z$:

$$\bar{\Phi}' = \Omega \begin{pmatrix} 1+|Z| & \mathrm{i}|Z| \\ \mathrm{i}|Z| & 1-|Z| \end{pmatrix},$$

whence the flatness is immediately apparent.

To conclude, the evolution of the wave packet in an electromagnetic field of a sufficiently general form is described by the nonlinear matrix equations, either (A2.4) or (A2.5), of the Riccati type. These equations are applicable to the description of the evolution of wave packets in a broad class of vacuum devices.

## References


1. Schottky W *Ann. Phys.* (Leipzig) **57** 541 (1918)
2. Glauber R J "Optical coherence and statistics of photons", in *Quantum Optics and Electronics* (Eds C DeWitt, A Blaudin, C Cohen-Tannoudji) (New York: Gordon and Breach, 1965) [Translated into Russian (Moscow: Mir, 1966) p. 91]
3. Loudon R *The Quantum Theory of Light* (Oxford: Clarendon Press, 1973) [Translated into Russian (Moscow: Mir, 1976)]
4. Perina J *Coherence of Light* (London: Van Nostrand Reinhold, 1972) [Translated into Russian (Moscow: Mir, 1974)]
5. Scully M O, Zubairy M S *Quantum Optics* (Cambridge: Cambridge Univ. Press, 1997)
6. Bykov V P, Gerasimov A V *Dokl. Ross. Akad. Nauk* **328** 50 (1993) [*Phys. Dokl.* **38** 35 (1993)]; Bykov V P, Gerasimov A V, Turin V O *Usp. Fiz. Nauk* **165** 955 (1995) [*Phys. Usp.* **38** 911 (1995)]; *Ann. Fond. Louis de Broglie* **20** 331 (1995); *Laser Phys.* **5** 841 (1995)
7. Wigner E *Phys. Rev.* **46** 1002 (1934); *Trans. Faraday Soc.* **34** 678 (1938)
8. Akhiezer A I, Berestetskii V B *Kvantovaya Elektrodinamika* (Quantum Electrodynamics) 4th ed. (Moscow: Nauka, 1981) [Translated into English from the 2nd Russian edition (New York: Interscience Publ., 1965)]
9. Bykov V P, Tatarskii V I *Zh. Eksp. Teor. Fiz.* **96** 528 (1989) [*Sov. Phys. JETP* **69** 299 (1989)]; Bykov V P, Tatarskii V I *Phys. Lett. A* **136** 77 (1989)
10. Von Neumann J *Mathematische Grundlagen der Quantenmechanik* (Berlin: J. Springer, 1932) [Translated into English: *Mathematical Foundations of Quantum Mechanics* (Princeton, NJ: Princeton Univ. Press, 1955); translated into Russian (Moscow: Nauka, 1964)]
11. Bykov V P *J. Russ. Laser Res.* **18** 260 (1997)
12. Bykov V P *Dokl. Akad. Nauk SSSR* **300** 1353 (1988) [*Sov. Phys. Dokl.* **33** 418 (1988)]; Bykov V P, Gerasimov A V, Preprint ICTP, IC/92/194 (1992)
13. Rivlin L A *Pis'ma Zh. Eksp. Teor. Fiz.* **13** 362 (1971) [*JETP Lett.* **13** 259 (1971)]
14. Arnold V I *Teoriya Katastrof* (The Theory of Catastrophes) 3rd ed. (Moscow: Nauka, 1990) [Translated into English: *Catastrophe Theory* (Berlin: Springer-Verlag, 1992)]
15. Monastyrskii M A *Prikl. Fiz.* (3) 7 (1996)
16. Bykov V P *Pis'ma Zh. Eksp. Teor. Fiz.* **64** 515 (1996) [*JETP Lett.* **64** 561 (1996)]
17. Bykov V P et al. *Pis'ma Zh. Eksp. Teor. Fiz.* **63** 408 (1996) [*JETP Lett.* **63** 429 (1996)]
18. Bykov V P, Turin V O *Laser Phys.* **7** 984 (1997); **8** 1039 (1998)
19. Bloembergen N *Phys. Rev. Lett.* **2** 84 (1959)
20. Karlov N V, Manenkov A A *Kvantovye Usiliteli* (Itogi Nauki. Radiofizika 1964 – 1965 gg.) (Quantum Amplifiers. Summary of Research. Radiophysics 1964 – 1965) (Moscow: VINITI, 1966)
21. Bykov V P, Dubrovich V K *Kratk. Soobshch. Fiz.* (9) 11 (1989)
22. Bykov V P *Laser Phys.* **9** 923 (1999); *Kvantovaya Elektron.* **29** 258 (1999) [*Quantum Electron.* **29** 1097 (1999)]; *Kratk. Soobshch. Fiz.* (7) 10 (1999) [*Bull. Lebedev Phys. Inst.* (7) 7 (1999)]; Preprint IOFAN No. 6 (Moscow: General Physics Institute of the Russian Academy of Sciences, 1999)
23. Zverev G M et al. *Lazery na Alyumoittrievom Granate s Neodimom* (Neodymium-Doped Yttrium-Aluminium Garnet Lasers) (Ed. N V Efimova) (Moscow: Radio i Svyaz', 1985)